The Plant Cell, Vol. 29: 1316–1334, June 2017, www.plantcell.org © 2017 ASPB.

The Jasmonate-Activated Transcription Factor MdMYC2 Regulates *ETHYLENE RESPONSE FACTOR* and Ethylene Biosynthetic Genes to Promote Ethylene Biosynthesis during Apple Fruit Ripening[OPEN]

Tong Li, Yaxiu Xu, Lichao Zhang, Yinglin Ji, Dongmei Tan, Hui Yuan, and Aide Wang[1]

College of Horticulture, Shenyang Agricultural University, Shenyang 110866, China

ORCID IDs: 0000-0002-8988-234X (T.L.); 0000-0002-7034-7021 (A.W.)

The plant hormone ethylene is critical for ripening in climacteric fruits, including apple (*Malus domestica*). Jasmonate (JA) promotes ethylene biosynthesis in apple fruit, but the underlying molecular mechanism is unclear. Here, we found that JA-induced ethylene production in apple fruit is dependent on the expression of *MdACS1*, an ACC synthase gene involved in ethylene biosynthesis. The expression of *MdMYC2*, encoding a transcription factor involved in the JA signaling pathway, was enhanced by MeJA treatment in apple fruits, and MdMYC2 directly bound to the promoters of both *MdACS1* and the ACC oxidase gene *MdACO1* and enhanced their transcription. Furthermore, MdMYC2 bound to the promoter of *MdERF3*, encoding a transcription factor involved in the ethylene-signaling pathway, thereby activating *MdACS1* transcription. We also found that MdMYC2 interacted with MdERF2, a suppressor of *MdERF3* and *MdACS1*. This protein interaction prevented MdERF2 from interacting with MdERF3 and from binding to the *MdACS1* promoter, leading to increased transcription of *MdACS1*. Collectively, these results indicate that JA promotes ethylene biosynthesis through the regulation of MdERFs and ethylene biosynthetic genes by MdMYC2.

INTRODUCTION

The ripening of fleshy fruits, which is widely studied due to its importance to the human diet (Adams-Phillips et al., 2004), typically involves textural changes and increased accumulation of color pigments, sugars, and volatile compounds (Klee and Giovannoni, 2011). Fruit ripening is influenced by internal and external cues, including light and temperature, as well as hormones, the most well studied of which is ethylene, particularly in climacteric fruit (Adams-Phillips et al., 2004).

Ethylene biosynthesis is essential for the ripening of climacteric fruit (Giovannoni, 2004). This process has been studied in many species, including the climacteric fruit, apple (*Malus domestica*) (Gapper et al., 2013; Seymour et al., 2013). Ethylene biosynthesis starts with the formation of ACC (1-aminocyclopropane-1-carboxylic acid) by the enzyme ACC synthase (ACS; EC 4.1.1.14) from *S*-adenosyl methionine; ACC is then oxidized by ACC oxidase (ACO) to form ethylene. These processes represent two key steps in the Yang cycle (Yang and Hoffman, 1984), with ACS generally cited as being the rate-limiting enzyme (Kende, 1993). During the signal transduction process, ethylene is detected by its receptors and the signal is transmitted downstream through several components, including CONSTITUTIVE TRIPLE RESPONSE1 and ETHYLENE INSENSITIVE2 (EIN2). A positive signal is then delivered to the primary transcription factor EIN3/EIN3-like, which induces the secondary transcription factor, ETHYLENE RESPONSE FACTOR (ERF), which in turn activates the expression of downstream ethylene-responsive genes (Lin et al., 2009; Klee and Giovannoni, 2011).

The importance of *ACS* or *ACO* genes in fruit ripening has been well documented. For example, silencing of *MdACS1* (Dandekari et al., 2004) or *MdACO1* in transgenic apple fruit blocks ethylene production (Schaffer et al., 2007). Moreover, many studies have shown that ethylene biosynthesis is regulated at the transcriptional level. Examples include the *MADS-box* gene, *RIPENING INHIBITOR*, an important regulator of fruit ripening, which binds to the CArG motif of the tomato (*Solanum lycopersicum*) *LeACS2* promoter (Ito et al., 2008), and in banana (*Musa acuminata*), in which MaERF11 binds to the promoter of *MaACO1* and suppress its expression (Han et al., 2016). In apple, MdMADS8 binds to the promoters of both *MdACS1* and *MdACO1* and activates their expression, while silencing of *MdMADS8* leads to a decrease in ethylene production (Ireland et al., 2013). Moreover, two ERFs, MdERF2 and MdERF3, bind to the DRE (dehydration-related element) motif in the *MdACS1* promoter; MdERF2 suppresses *MdACS1* expression, whereas MdERF3 promoting its expression (Li et al., 2016). These findings suggest that transcriptional regulation is an important factor in ethylene biosynthesis.

Jasmonate (JA) also plays important roles in fruit ripening (Srivastava and Handa, 2005; Barry and Giovannoni, 2007). After its biosynthesis, JA is conjugated with Ile to form the bioactive hormone JA-Ile (Kazan and Manners, 2013; Zhang et al., 2014). JASMONATE ZIM-DOMAIN PROTEIN (JAZ), which is degraded after JA treatment, interacts with a number of transcription factors, including MYC (Fernández-Calvo et al., 2011), and represses their

[1] Address correspondence to adwang333@163.com.
The author responsible for distribution of materials integral to the findings presented in this article in accordance with the policy described in the Instructions for Authors (www.plantcell.org) is: Aide Wang (adwang333@163.com).
[OPEN] Articles can be viewed without a subscription.
www.plantcell.org/cgi/doi/10.1105/tpc.17.00349

transcription (Pauwels et al., 2010; Zhu et al., 2011; Kazan and Manners, 2013). The F-box protein CORONATINE INSENSITIVE1 and JAZ together constitute the coreceptor for JA-Ile (Sheard et al., 2010). JA-Ile is sensed by this coreceptor, leading to JAZ degradation and the release of the abovementioned transcription factors; these transcription factors activate their downstream genes, resulting in the JA responses (Kazan and Manners, 2013). MYC is considered to function as the master regulator of the JA signaling pathway (Kazan and Manners, 2013; Zhang et al., 2014).

Many studies involving various species have been performed to elucidate the role of JA in fruit ripening (Saniewski et al., 1987; Fan et al., 1997; Kondo et al., 2009; Concha et al., 2013; Khan and Singh, 2015). For example, Kondo et al. (2000) reported that endogenous JA levels increase in apple fruit during maturation. Additionally, the application of JA to fruits results in increased ethylene production in tomato (Saniewski and Czapski, 1985; Saniewski et al., 1987), apple (Fan et al., 1997; Fan et al., 1998; Kondo et al., 2009), plum (*Prunus salicina*) (Khan and Singh, 2015), and mango (*Mangifera indica*) (Lalel et al., 2015). However, little is known about the mechanism by which JA promotes ethylene production, such as enhancing the expression of ethylene signaling genes (Saniewski et al., 1987; Fan et al., 1998; Kondo et al., 2009; Khan and Singh, 2015), thereby promoting the expression of ethylene biosynthetic genes and ethylene production during fruit ripening.

In this study, we cloned the MYC transcription factor gene *MdMYC2*, an important regulator of the JA signaling pathway, from apple fruit. The expression of *MdMYC2* was markedly induced in fruit treated with JA, and MdMYC2 upregulated both *MdACS1* and *MdACO1* transcription by binding to their promoters and by upregulating the expression of *MdERF3*, which promotes *MdACS1* transcription. Moreover, MdMYC2 and MdERF2 were found to interact, resulting in the promotion of *MdACS1* transcription. These results provide important insights into the molecular basis by which JA promotes ethylene biosynthesis during apple fruit ripening.

RESULTS

JA Promotes the Expression of *MdACS1* and *MdACO1* and Ethylene Production in Apple Fruit

MdACS1 and *MdACO1* were shown to be essential for ethylene biosynthesis in apple fruit, since ethylene production is blocked in *MdACS1*- or *MdACO1*-supressed apple fruit (Dandekari et al., 2004; Schaffer et al., 2007). *MdACS1* expression is first detected at 140 DAFB (days after full bloom) in the 'Golden Delicious' (GD) apple cultivar (Li et al., 2015). In this study, GD apple fruits were harvested at 110 DAFB (immature stage), treated with methyl jasmonate (MeJA), and stored at room temperature for 20 d. *MdACS1* was not expressed in untreated or in MeJA-treated fruits during the storage period (Supplemental Figure 1A), and MeJA treatment did not significantly alter ethylene production (Supplemental Figure 1C); however, *MdACO1* was expressed and was induced by MeJA treatment during this period (Supplemental Figure 1B). These results suggest that JA cannot induce ethylene production in apple fruits at an immature stage when *MdACS1* expression is not initiated. When fruits were harvested at 125 DAFB, treated with MeJA, and stored at room temperature for 20 d (Figure 1A), *MdACS1* was not expressed from the time of harvest to 10 DAH (days after harvest), and MeJA treatment did not induce its expression during this period (Figure 1C). However, beginning at 15 DAH, *MdACS1* expression was detected in untreated fruit, and MeJA treatment promoted its expression from this time point onward (Figure 1C). Interestingly, the pattern of ethylene production paralleled the expression pattern of *MdACS1* in both untreated and MeJA-treated fruits (Figure 1D). Although *MdACO1* was induced by MeJA treatment from 5 DAH and throughout storage period (Figure 1B), its expression pattern did not correlate with the induction of ethylene production (Figures 1B and 1D). In addition, fruits were harvested at 140 DAFB, treated with MeJA or 1-MCP (1-methylcyclopropene; an ethylene antagonist), or with 1-MCP followed by MeJA, and stored at room temperature for 20 d (Figure 1E). The expression of both *MdACS1* and *MdACO1* was initiated immediately after harvest, and MeJA treatment significantly promoted their expression during the storage period. In contrast, 1-MCP treatment blocked the expression of both genes, and the application of MeJA did not induce *MdACS1* expression in 1-MCP-treated fruit (Figures 1F and 1G). The pattern of ethylene production was the same as that of *MdACS1* expression after the various treatments (Figure 1H). These results suggest that the expression of ethylene biosynthetic genes, and particularly *MdACS1*, is necessary for JA to promote ethylene production in apple fruit.

Next, we silenced *MdACS1* in apple fruit calli by antisense technology using *Agrobacterium tumefaciens*-mediated transformation (Figure 1I). *MdACS1*-silenced calli (MdACS1-AN) showed significantly lower ethylene production than the control calli after treatment with MeJA (Figure 1J), further demonstrating the importance of *MdACS1* in JA-induced ethylene biosynthesis.

MdMYC2 Is Essential for JA-Induced Ethylene Biosynthesis in Apple Fruit

The increased expression of both *MdACS1* and *MdACO1* in MeJA-treated fruit suggested that the action of JA in promoting ethylene biosynthesis involves transcriptional regulation. Since MYC transcription factors are key transcription factors in the JA signaling pathway (Kazan and Manners, 2013), we targeted apple *MYC* genes for further analysis. A review of the apple genome sequence (https://www.rosaceae.org/) revealed four *MYC* genes, only one of which, *MdMYC2*, was expressed in apple fruit (Supplemental Figure 2). MdMYC2 was predicted to contain domains that are shared with its homologs from *Arabidopsis thaliana* and tobacco (*Nicotiana tabacum*) (Supplemental Figure 3). *MdMYC2* expression was induced in apple fruits by MeJA treatment (Figure 2A; Supplemental Figure 2).

To address the importance of MdMYC2 in JA-induced ethylene biosynthesis, we silenced *MdMYC2* expression in apple fruit calli using Agrobacterium-mediated transformation. Eight transgenic lines were generated, of which lines #1, #4, and #5 showed substantially suppressed expression of *MdMYC2* at both the transcript and protein levels (Figure 2B). We then treated the calli with MeJA and evaluated *MdACS1* and *MdACO1* expression and ethylene production. The expression levels of both *MdACS1* and *MdACO1* were markedly lower in *MdMYC2*-supressed calli than in control calli (Figure 2C), and ethylene production showed the same pattern as the change in *MdACS1* and *MdACO1* expression (Figure 2D), demonstrating that MdMYC2 is required for

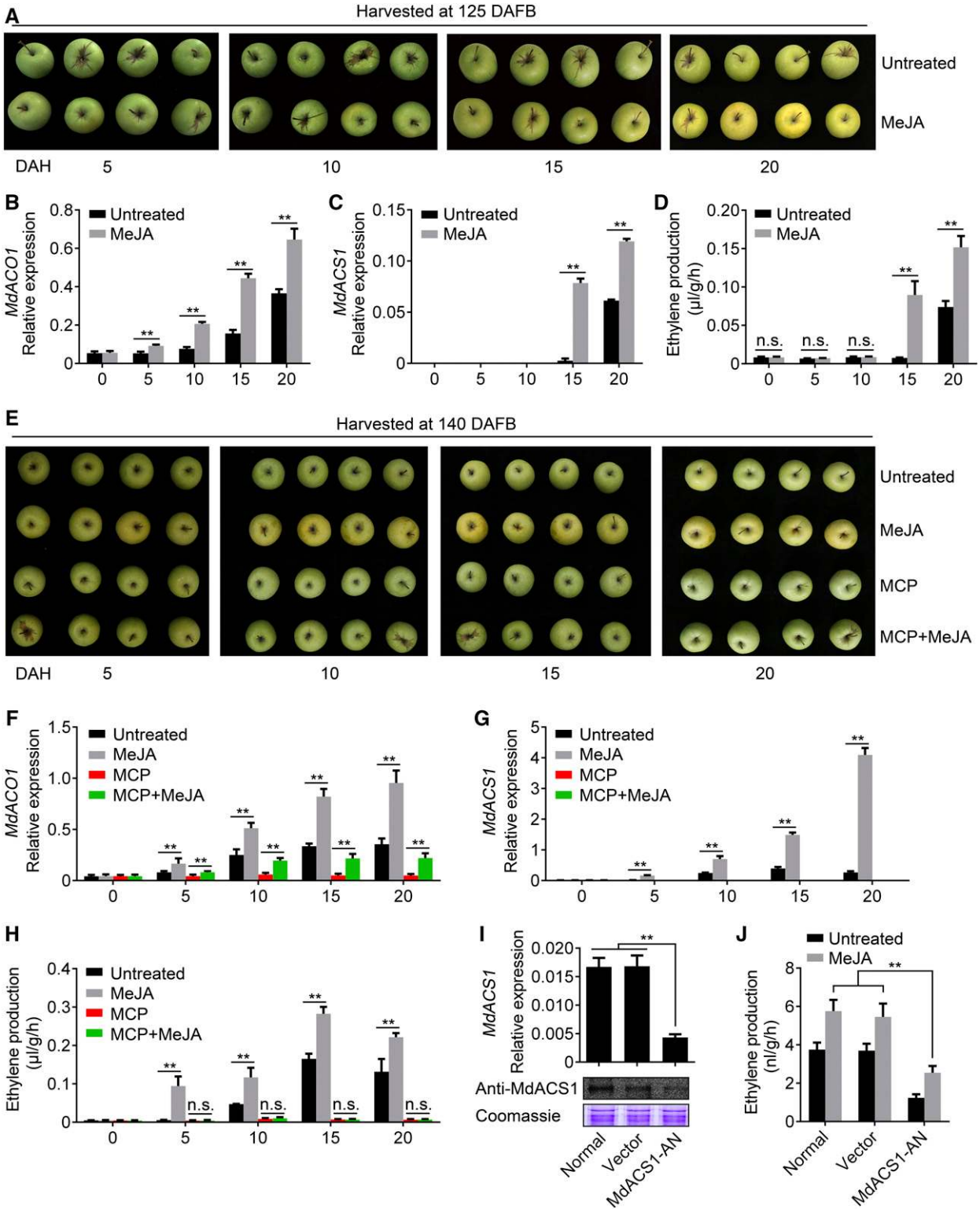

Figure 1. JA-Induced Ethylene Biosynthesis Is Dependent on *MdACS1* Expression.

(A) to **(D)** GD apple fruits were harvested at 125 DAFB, treated with MeJA, and stored at room temperature for 20 d **(A)**. The expression levels of *MdACO1* **(B)** and *MdACS1* **(C)** were investigated by qRT-PCR, and ethylene production was measured **(D)**. Untreated, intact fruits not receiving any treatment; MeJA, fruits treated with MeJA. Numbers under the *x* axes of **(B)** to **(D)** indicate the DAH.

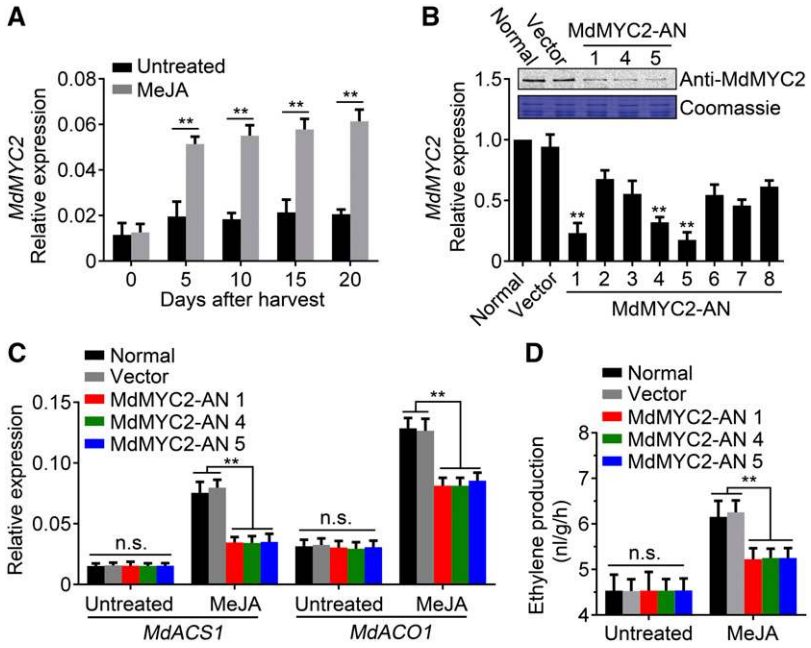

Figure 2. MdMYC2 Is Required for JA-Induced Ethylene Biosynthesis in Apple Calli.

(A) *MdMYC2* expression was investigated by qRT-PCR in apple fruit; untreated or treated with MeJA. Fruit tissues were the same as in Figure 1E.
(B) to **(D)** *MdMYC2* expression was silenced in apple fruit calli (MdMYC2-AN) by Agrobacterium infection as described in Methods. *MdMYC2* expression was investigated by qRT-PCR and immunoblot analysis **(B)**. A Coomassie-stained SDS-PAGE gel (Coomassie) was used to confirm equal sample loading. The expression levels of *MdACS1* and *MdACO1* were investigated by qRT-PCR in *MdMYC2*-suppressed calli **(C)**. *MdMYC2*-suppressed calli were treated with MeJA as described in Methods, and the ethylene production was measured **(D)**. Numbers under the *x* axis of **(B)** indicate the line numbers of *MdMYC2*-suppressed calli. Noninfected calli (Normal) and calli infected with empty vector (Vector) were used as controls. For qRT-PCR analysis, three biological replicates were performed as described in the legend of Figure 1. Values represent means ± SE. Statistical significance was determined using a Student's *t* test (**P < 0.01). n.s., no significant difference.

JA-induced ethylene biosynthesis and suggesting that it might regulate the transcription of both *MdACS1* and *MdACO1*.

MdMYC2 Enhances the Transcription of Both *MdACS1* and *MdACO1* by Binding to Their Promoters

We investigated the binding of MdMYC2 to the *MdACS1* promoter using a yeast one-hybrid (Y1H) assay (Figure 3A). Various fragments of the promoter were tested, and we saw that MdMYC2 bound to the fragment containing the G-box motif (Figure 3A). To further confirm the interaction, we purified the full-length MdMYC2 protein and performed an electrophoretic mobility shift assay (EMSA) with fragments of biotin-labeled *MdACS1* promoter containing the G-box motif as the labeled probe. MdMYC2 bound to the *MdACS1* promoter (Figure 3B, lane 1), and when an unlabeled probe containing two mutated nucleotides was added as a competitor, the binding of MdMYC2 to the *MdACS1* promoter was not affected (Figure 3B, lane 2). This result indicates that MdMYC2 binds to the G-box motif of the *MdACS1* promoter.

Figure 1. (continued).

(E) to **(H)** GD fruits were harvested at 140 DAFB, treated with MeJA, 1-MCP, or 1-MCP plus MeJA and stored at room temperature for 20 d **(E)**. The expression levels of *MdACO1* **(F)** and *MdACS1* **(G)** were investigated by qRT-PCR, and ethylene production was measured **(H)**. Untreated, intact fruits not receiving any treatment; MeJA, fruits treated with MeJA; MCP, fruits treated with 1-MCP; MCP+MeJA, fruits treated with 1-MCP for 12 h followed by MeJA treatment. Numbers under the *x* axes of **(F)** to **(H)** indicate the DAH.
(I) and **(J)** *MdACS1* expression was silenced in apple fruit calli (MdACS1-AN) by Agrobacterium infection. *MdACS1* expression was investigated by qRT-PCR and immunoblot analysis **(I)**. A Coomassie-stained SDS-PAGE gel (Coomassie) was used to confirm equal sample loading. *MdACS1*-suppressed calli were treated with MeJA, and ethylene production was measured **(J)**. Noninfected calli (Normal) and calli infected with empty vector (Vector) were used as controls. For qRT-PCR, fruits sampled at each sampling point were divided into three groups (two fruits per group). The fruit flesh in each group was evenly mixed for RNA extraction. RNA extracted from each group was used as one biological replicate in qRT-PCR. A total of three biological replicates were analyzed. For calli samples, each successfully infected line was grown on three separate plates containing solid medium. The calli grown on each plate were used as one biological replicate. A total of three biological replicates were analyzed. Values represent means ± SE. Statistical significance was determined using a Student's *t* test (**P < 0.01). n.s., no significant difference.

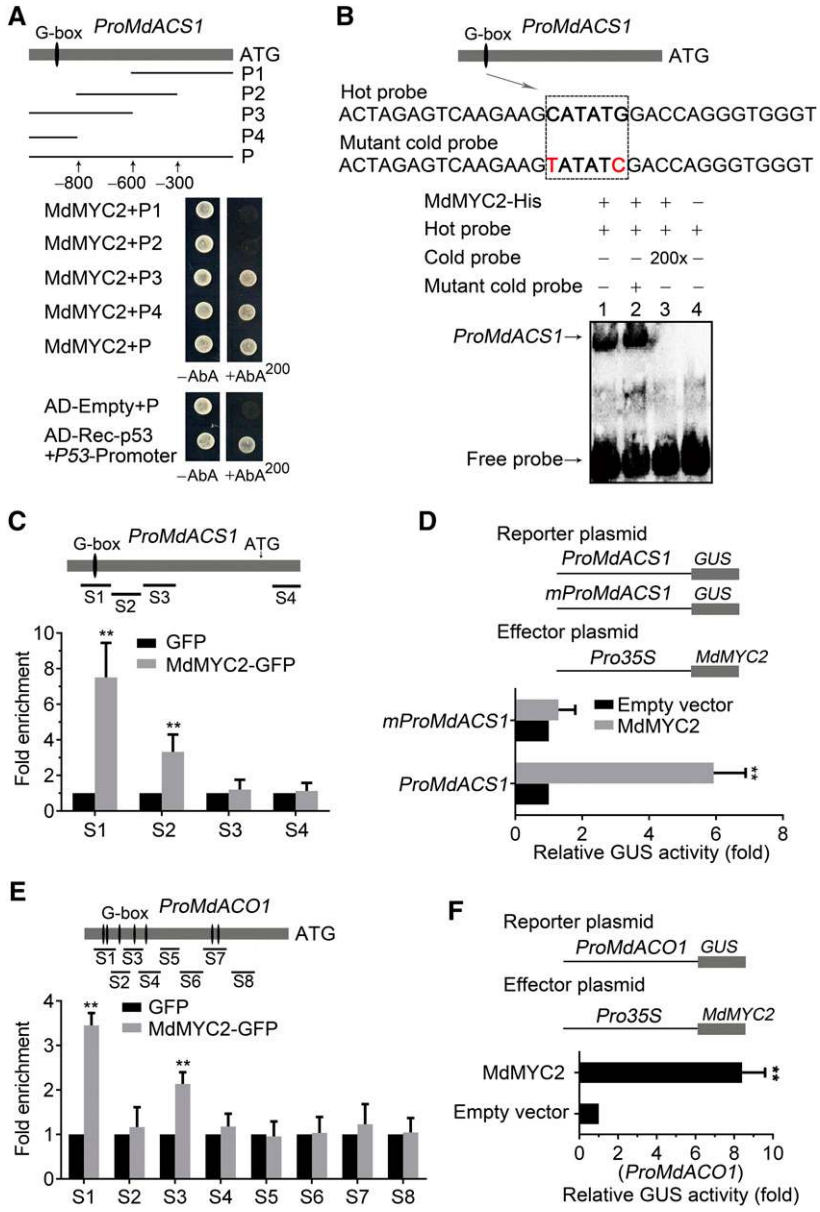

Figure 3. MdMYC2 Promotes Both *MdACS1* and *MdACO1* Transcription.

(A) Y1H analysis showing that MdMYC2 binds to the *MdACS1* promoter fragment (*ProMdACS1*) containing the G-box motif (−1101). The promoter of *MdACS1* was divided into four fragments (P1 to P4). AbA (Aureobasidin A), a yeast cell growth inhibitor, was used as a screening marker. The basal concentration of AbA was 200 ng/mL. Rec-P53 and the *P53*-promoter, whose interaction has been confirmed, acted as positive controls. The empty vector and the *MdACS1* promoter (P; 1191 bp) were used as negative controls.

(B) EMSA analysis showing that MdMYC2 binds to the G-box motif of the *MdACS1* promoter. The hot probe was a biotin-labeled fragment of the *MdACS1* promoter containing the G-box motif, and the cold probe was a nonlabeled competitive probe (200-fold that of the hot probe). The mutant cold probe was the unlabeled hot probe sequence with two nucleotides mutated. His-tagged MdMYC2 was purified.

(C) ChIP-PCR showing the in vivo binding of MdMYC2 to the *MdACS1* promoter. Cross-linked chromatin samples were extracted from MdMYC2-GFP-overexpressing fruit calli and precipitated with an anti-GFP antibody. Eluted DNA was used to amplify the sequences neighboring the G-box by qPCR. Four regions (S1–S4) were investigated. Fruit calli overexpressing the GFP sequence were used as negative controls. The ChIP assay was repeated three times and the enriched DNA fragments in each ChIP were used as one biological replicate for qPCR. Values represent means ± SE. Asterisks indicate significantly different values (**$P < 0.01$).

(D) GUS activity analysis showing that MdMYC2 activates the *MdACS1* promoter. The MdMYC2 effector vector, together with the reporter vector containing the *MdACS1* promoter or a mutated promoter (with two nucleotides mutated as shown in **[B]**, *mProMdACS1*), were infiltrated into wild tobacco leaves to

To confirm that MdMYC2 bound to the promoter of *MdACS1* in vivo, we conducted a chromatin immunoprecipitation (ChIP)-PCR assay. The coding sequence (CDS) of *MdMYC2* fused to a sequence encoding a GFP peptide tag was overexpressed in apple fruit calli. The presence of MdMYC2 substantially enhanced the PCR-based detection of the *MdACS1* promoter (Figure 3C), indicating that MdMYC2 binds to the *MdACS1* promoter in vivo.

We investigated the regulation of the *MdACS1* promoter by MdMYC2 using a GUS transactivation assay in wild tobacco (*Nicotiana benthamiana*) leaves involving cotransformation with the *Pro35S:MdMYC2* and *ProMdACS1:GUS* constructs (Figure 3D). When *Pro35S:MdMYC2* was cotransformed with *ProMdACS1: GUS*, *MdACS1* promoter activity increased, while the activity of a mutated *MdACS1* promoter (*ProMdACS1mG-box*), in which the G-box was mutated (Figure 3B) was not altered (Figure 3D).

Since *MdACO1* also contains G-box motifs in its promoter, we conducted a ChIP-PCR assay to confirm the in vivo binding of MdMYC2 to the *MdACO1* promoter. The presence of MdMYC2 substantially enhanced the PCR-based detection of the *MdACO1* promoter (Figure 3E), indicating that MdMYC2 binds to the *MdACO1* promoter in vivo. We also investigated the regulation of the *MdACO1* promoter by MdMYC2 using a GUS transactivation assay in wild tobacco leaves. When *Pro35S:MdMYC2* was co-transformed with *ProMdACO1:GUS*, the activity of the *MdACO1* promoter increased (Figure 3F). These results are consistent with the notion that MdMYC2 promotes the transcription of both *MdACS1* and *MdACO1*.

MdMYC2 Enhances the Transcription of *MdERF3*, Which Positively Regulates the *MdACS1* Promoter

Previously, we reported that ERF transcription factors regulate the expression of *MdACS1* (Li et al., 2016), and in this study, we examined the expression of three *ERF*s, *MdERF1*, *2*, and *3* (Wang et al., 2007; Li et al., 2016). The expression of *MdERF1* and *2* in apple fruit was not affected by MeJA treatment (Figures 4A and 4B), but the expression of *MdERF3* was substantially induced by this treatment (Figure 4C). In addition, the expression of *MdERF3* in *MdMYC2*-suppressed apple calli treated with MeJA was significantly lower than that in the control calli (Figure 4D), showing the same pattern as that for *MdACS1* (Figure 2C). We previously reported (Li et al., 2016) that MdERF3 is a transcriptional activator that induces *MdACS1* transcription by binding to its promoter; thus, we reasoned that MdMYC2 might enhance *MdERF3* expression, subsequently leading to a higher level of *MdACS1* expression. We identified two MdMYC2 binding sites (G-boxes) in the *MdERF3* promoter and examined the binding of MdMYC2 to the *MdERF3* promoter using a Y1H assay. MdMYC2 bound to an *MdERF3* promoter region containing the G-boxes (Figure 5A). We performed an EMSA to confirm this interaction, finding that MdMYC2 bound to both G-boxes (Figure 5B, lanes 3 and 5) and that when mutated unlabeled probes were added as competitors, the binding was not affected (Figure 5B, lanes 4 and 6). To confirm the in vivo binding of MdMYC2 to the *MdERF3* promoter, we performed a ChIP-PCR assay, which revealed that the presence of MdMYC2 substantially enhanced the PCR-based detection of the *MdERF3* promoter (Figure 5C), indicating that MdMYC2 binds to the *MdERF3* promoter in vivo. Taken together, these results are consistent with the notion that MdMYC2 regulates *MdERF3* transcription by interacting with its G-box motifs, thereby influencing the expression of *MdACS1*. Finally, ChIP-PCR analysis showed that MdMYC2 could not bind to the promoter of *MdERF1* or *2* (Supplemental Figure 4).

We then investigated the regulation of the *MdERF3* promoter by MdMYC2 using a GUS transactivation assay in wild tobacco leaves. When *Pro35S:MdMYC2* was cotransformed with *ProMdERF3:GUS*, enhanced *MdERF3* promoter activity was detected, even when one of the G-box motifs was mutated (Figure 5D). These results indicate that MdMYC2 can enhance the transcription of *MdERF3*, thereby leading to higher level of *MdACS1* expression.

The MdMYC2 binding site is only 31 bp downstream of the MdERF3 binding site in the *MdACS1* promoter (Supplemental Figure 5A), and we hypothesized that these two transcription factors might influence *MdACS1* expression by binding to each other's *cis*-elements. To investigate this possibility, we purified full-length recombinant MdMYC2 and MdERF3 proteins, as well as their binding domains (amino acids 500–600 for MdMYC2 and amino acids 140–200 for MdERF3), each of which included a His tag, and performed EMSA analyses. MdMYC2 and MdERF3 did not interfere with each other's binding to the *MdACS1* promoter (Supplemental Figures 5B and 5C).

Additionally, we speculated that MdMYC2 might regulate the transcription of *MdACO1* indirectly through MdERF3. However, we did not find an ERF binding site in the *MdACO1* promoter (defined here as 2000 bp upstream of the translational start site). Moreover, ChIP-PCR analysis showed that MdERF3 could not bind the *MdACO1* promoter in vivo (Supplemental Figure 6). Therefore, the transcription of *MdACO1* is not regulated by MdERF3; therefore, MdMYC2 does not regulate *MdACO1* expression through MdERF3.

Figure 3. (continued).

analyze the regulation of GUS activity. Three independent transfection experiments were performed. Values represent means ± SE. Asterisks indicate significantly different values (**P < 0.01).

(E) ChIP-PCR showing the in vivo binding of MdMYC2 to the *MdACO1* promoter (1240 bp). ChIP-PCR was conducted as in **(C)**. Eight regions (S1–S8) of the *MdACO1* promoter were investigated. Fruit calli overexpressing the GFP sequence were used as negative controls. The ChIP assay was repeated three times, and the enriched DNA fragments in each ChIP assay were used as one biological replicate for qPCR. Values represent means ± SE. Asterisks indicate significantly different values (**P < 0.01).

(F) GUS activity analysis showing that MdMYC2 activates the *MdACO1* promoter. The MdMYC2 effector vector and the reporter vector containing the *MdACO1* promoter were infiltrated into wild tobacco leaves to analyze the regulation of GUS activity. Three independent transfection experiments were performed. Values represent means ± SE. Asterisks indicate significantly different values (**P < 0.01).

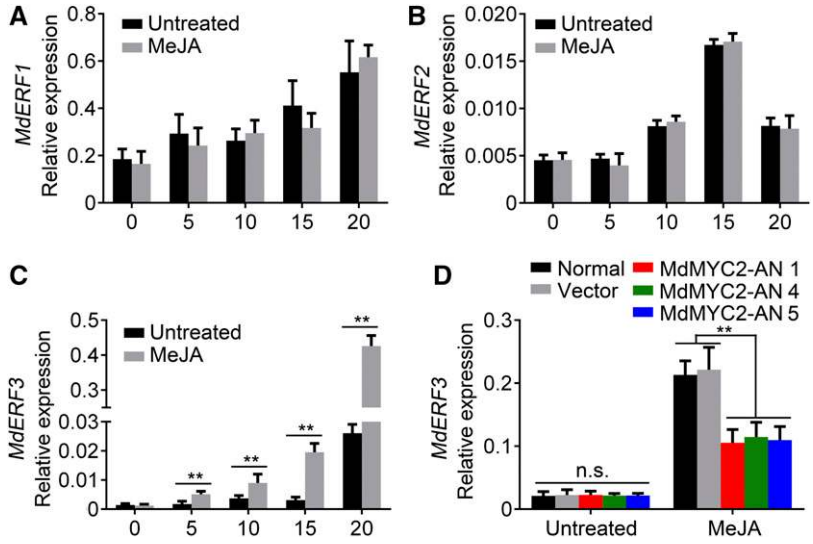

Figure 4. *MdERF3* Expression Is Promoted by MeJA Treatment.

(A) to **(C)** Expression levels of *MdERF1* **(A)**, *MdERF2* **(B)**, and *MdERF3* **(C)** were investigated by qRT-PCR in untreated or MeJA-treated apple fruit. Fruit tissues were as in Figure 1E. Numbers under the *x* axis indicate the DAH.

(D) *MdMYC2*-suppressed calli (MdMYC2-AN) were treated with MeJA, and the *MdERF3* expression level was investigated by qRT-PCR. Noninfected calli (Normal) and calli infected with an empty vector (Vector) were used as the controls. For qRT-PCR, three biological replicates were analyzed as described in the legend of Figure 1. Values represent means ± SE. Statistical significance was determined using a Student's *t* test (**P < 0.01). n.s., no significant difference.

MdMYC2 Enhances the Transcription of *MdACS1* by Interacting with MdERF2

Although the expression pattern of *MdERF1* and *2* in apple fruit was not affected by MeJA treatment (Figures 4A and 4B), the corresponding proteins might still interact with MdMYC2 and affect its regulation of *MdACS1*. We therefore investigated the interaction between MdMYC2 and the three MdERF proteins using a yeast two-hybrid (Y2H) assay. The result showed that MdMYC2 could interact with MdERF2, but not with MdERF1 or MdERF3, in yeast cells (Supplemental Figure 7). Moreover, when N-terminal or C-terminal regions of MdMYC2 were tested separately, only the N terminus (MdMYC2N) interacted with MdERF2 (Figure 6A). When MdERF2 was divided into three fragments (N terminus, ERF domain, and C terminus), the N terminus of MdMYC2 interacted with the N terminus of MdERF2 (MdERF2N) (Figure 6B). We then purified recombinant poly-histidine-tagged MdMYC2N (MdMYC2N-His) and recombinant glutathione *S*-transferase-tagged MdERF2N (MdERF2N-GST), MdERF2D (MdERF2D-GST), or MdERF2C (MdERF2C-GST) fusion proteins and performed a pull-down assay to confirm the interaction between MdMYC2N and MdERF2N (Figure 6C). Lastly, we transformed apple fruit calli with a construct harboring a sequence encoding a GFP tag fused to the *MdMYC2* CDS in order to perform a coimmunoprecipitation (co-IP) assay. MdERF2 protein was immunoprecipitated from extracts from the MdMYC2-GFP transgenic calli, but not from extracts from the GFP transgenic calli, using an anti-GFP antibody, confirming the in vivo interaction between MdMYC2 and MdERF2 (Figure 6D).

We previously showed that MdERF2 is a transcriptional repressor that binds to the *MdACS1* promoter and suppresses its expression (Li et al., 2016). Therefore, the MdMYC2-MdERF2 interaction might affect the binding of MdERF2 to the *MdACS1* promoter. To test this possibility, we purified the MdMYC2 and MdERF2 proteins and performed EMSA analysis with the *MdACS1* promoter only containing the DRE motif (MdERF2 binding site) as a probe. The MdERF2 protein alone bound to the *MdACS1* promoter, while MdMYC2 did not (Figure 7A, lanes 3 and 2), and when increasing amounts of MdMYC2 were added, the binding of MdERF2 to the *MdACS1* promoter gradually weakened (Figure 7A, lanes 4–6).

To investigate how the MdMYC2-MdERF2 interaction affects the activity of the *MdACS1* promoter, the CDSs of *MdMYC2* and *MdERF2* were ligated into the pRI101 vector under the control of the CaMV 35S promoter to generate the *Pro35S:MdMYC2* and *Pro35S:MdERF2* plasmids. The recombinant plasmids *Pro35S:MdMYC2* and *Pro35S:MdERF2* were used in a GUS transactivation assay in wild tobacco leaves. Specifically, we cotransformed the leaves with the *Pro35S:MdMYC2*/*Pro35S:MdERF2* plasmids together with the *ProMdACS1mG-box:GUS* plasmid, which has a *MdACS1* promoter containing a mutated G-box to avoid interference from MdMYC2 binding. The GUS activity level was significantly higher when *Pro35S:MdMYC2* and *Pro35S:MdERF2* were cotransformed together with *ProMdACS1mG-box:GUS* than after the single transformation of *Pro35S:MdERF2* and *ProMdACS1mG-box:GUS* (Figure 7B).

Since both MdMYC2 and MdERF2 can bind to the promoter of *MdACS1*, the MdMYC2-MdERF2 interaction might also affect the binding of MdMYC2 to the *MdACS1* promoter. To test this possibility, the purified MdMYC2 and MdERF2 proteins were used in an EMSA analysis with the *MdACS1* promoter only containing

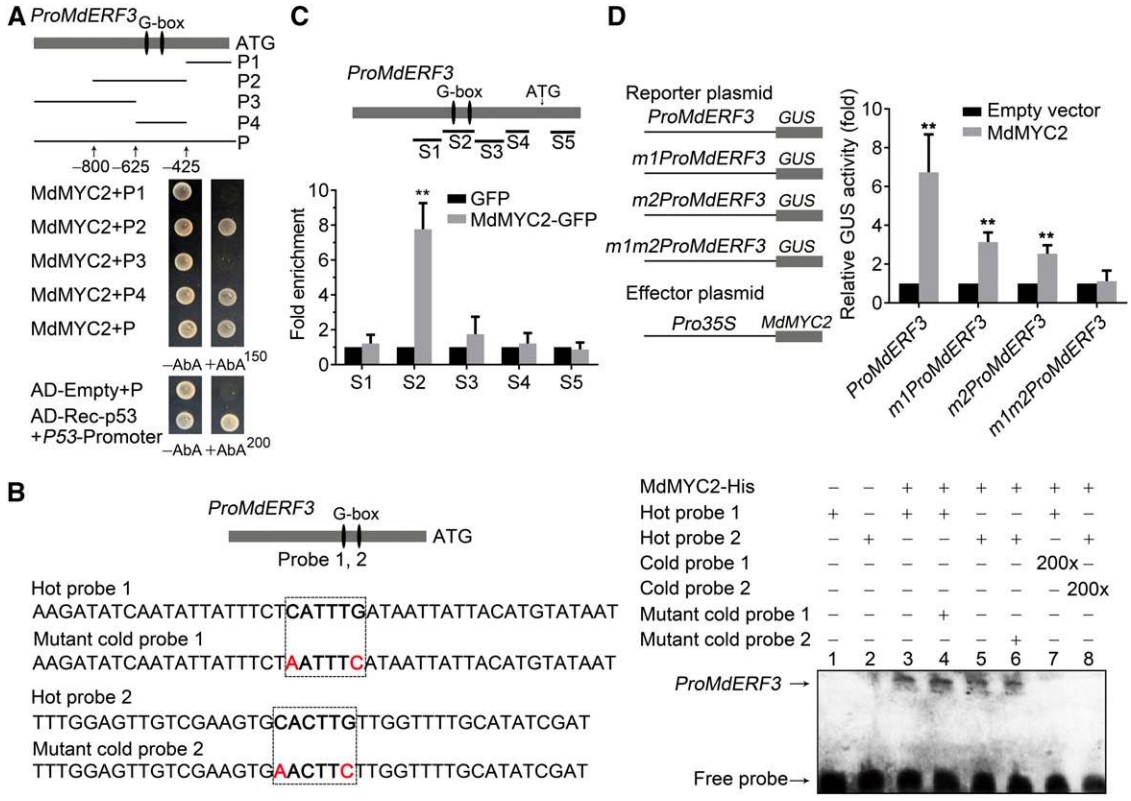

Figure 5. MdMYC2 Positively Regulates *MdERF3* Transcription.

(A) Y1H results showing that MdMYC2 binds to the promoter fragment of *MdERF3* containing the G-box motifs. The promoter of *MdERF3* was divided into four fragments (P1–P4). The basal concentration of AbA was 150 ng/mL. Rec-P53 and the *P53*-promoter were used as the positive controls. The empty vector and the *MdERF3* promoter (P; 1158 bp) were used as negative controls.

(B) EMSA results showing that MdMYC2 binds to the G-box motif of the *MdERF3* promoter. The hot probe was a biotin-labeled *MdERF3* promoter fragment containing two G-box motifs, and the cold probe was a nonlabeled competitive probe (200-fold that of the hot probe). A mutant cold probe was an unlabeled hot probe sequence with two mutated nucleotides. His-tagged MdMYC2 was purified.

(C) ChIP-PCR showing the in vivo binding of MdMYC2 to the *MdERF3* promoter. ChIP-PCR was performed as in Figure 3C. Five regions (S1–S5) were examined. Asterisks indicate significantly different values (**P < 0.01).

(D) GUS activity analysis showing that MdMYC2 induces the expression of *MdERF3*. The MdMYC2 effector vector, together with the reporter vector containing the *MdERF3* promoter or mutated promoters (with two nucleotides mutated in each G-box motif as shown in **[B]**, *m1m2ProMdERF3*), were infiltrated into wild tobacco leaves to assess the regulation of GUS activity. Three independent transfection experiments were performed. Values represent means ± SE. Asterisks indicate significantly different values (**P < 0.01).

the G-box motif (MdMYC2 binding site) as a probe. The binding of MdMYC2 to the *MdACS1* promoter gradually weakened when increasing amounts of MdERF2 were added (Supplemental Figure 8A, lanes 4–6), indicating that the interaction between MdMYC2 and MdERF2 inhibited the binding of MdMYC2 to the *MdACS1* promoter. The GUS transactivation assay also showed that the MdMYC2-MdERF2 interaction decreased the regulation of the *MdACS1* promoter by MdMYC2 (Supplemental Figure 8B). It is also possible that the MdMYC2-MdERF2 interaction influences the binding of MdMYC2 to the *MdACO1* promoter; indeed, the EMSA analysis and GUS transactivation assay showed that the effect was similar to that on the *MdACS1* promoter (Supplemental Figures 8C and 8D).

We previously showed that the N terminus of MdERF2 interacts with the binding domain of MdERF3 (amino acids 140–200), which is the region that binds to the *MdACS1* promoter (Li et al., 2016). This interaction inhibits the binding of MdERF3 to the *MdACS1* promoter, thereby repressing *MdACS1* transcription. We reasoned that the MdMYC2-MdERF2 interaction might affect the interaction between MdERF2 and MdERF3. To test this possibility, we performed a pull-down assay with purified recombinant poly histidine-tagged MdERF2 (MdERF2-His), a recombinant MdMYC2-maltose binding protein fusion (MdMYC2-MBP), and recombinant MdERF3 GST fusion protein (MdERF3-GST), where the latter was immobilized on a column and used to identify binding protein partners. MdERF2-His together with MdMYC2-MBP was incubated with MdERF3-GST, and an anti-His antibody was used to detect the immunoprecipitated fractions. When increasing amounts of MdMYC2-MBP were added, the amount of associated MdERF2 protein progressively decreased (Figure 7C, lanes 4–6), indicating that MdMYC2 competes with MdERF3 for binding to MdERF2.

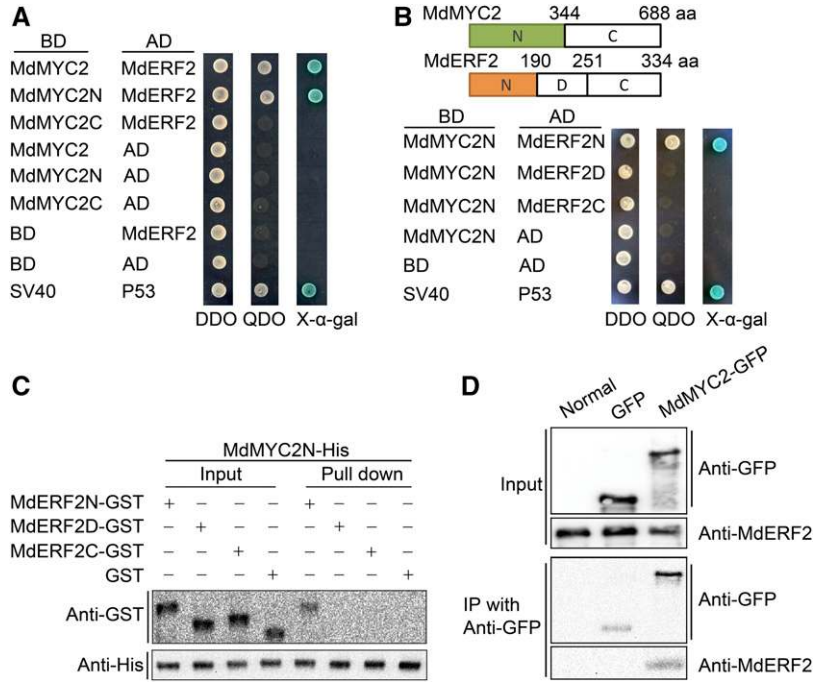

Figure 6. The MdMYC2 and MdERF2 Proteins Interact.

(A) MdMYC2 was divided into two fragments, and their interactions with MdERF2 were analyzed using a Y2H assay. *MdMYC2* fragments were ligated into the pGBKT7 vector (binding domain [BD]) and *MdERF2* into the pGADT7 vector (activation domain [AD]). DDO, SD medium lacking Trp and Leu; QDO, SD medium lacking Trp, Leu, His, and Ade; X-α-gal, QDO medium containing x-α-gal and AbA. The SV40 and P53 genes were used as the positive control, and AD and BD vectors as the negative control. Blue plaques indicate interaction between two proteins.

(B) MdERF2 was divided into three fragments, and their interactions with MdMYC2N were analyzed using a Y2H assay. MdERF2 fragments were ligated into the pGADT7 vector.

(C) The interactions between fragments of MdMCY2 and three fragments of MdERF2 were analyzed using a pull-down assay. Recombinant GST-tagged MdERF2 fragments (MdERF2N-, D-, and C-GST) and His-tagged MdMYC2N protein (MdMYC2N-His) was produced, and MdMYC2N-His was used in a pull-down analysis. GST- and His-antibodies were used for immunoblot analyses. The band detected by the GST antibody in the pull-down protein sample indicates the interaction between MdMYC2N and MdERF2N.

(D) The interaction between MdMYC2 and MdERF2 was confirmed with a co-IP assay. MdMYC2 fused to a GFP tag was overexpressed in apple fruit calli (MdMYC2-GFP) and a GFP antibody was used for immunoprecipitation analysis. GFP and MdERF2 antibodies were used in an immunoblot analysis. Intact calli (Normal) were used as a control. The band detected by the MdERF2 antibody in the precipitated protein sample indicates the interaction between MdMYC2 and MdERF2.

We then conducted a firefly luciferase (Luc) complementation imaging assay to confirm this result in vivo. Constructs containing MdERF2 fused with the N terminus of Luc (MdERF2-nLuc), or the C terminus of Luc fused with MdERF3 (cLuc-MdERF3), as well as MdMYC2 (pRI101-MdMYC2) were coinfiltrated into wild tobacco leaves to transiently express the corresponding fusion proteins. A strong luminescence signal was detected in the MdERF2-nLuc/cLuc-MdERF3 coexpression region (Figure 7D, region 1) but not in the negative controls (Figure 7D, regions 4–6), and increasing amounts of added pRI101-MdMYC2 showed an inverse relationship with the strength of the luminescence signal (Figure 7D, region 2). Greater amounts of added pRI101-MdMYC2 resulted in weaker luminescence signals (Figure 7D, region 3). These results indicate that the MdMYC2-MdERF2 interaction interferes with binding of MdERF2 to MdERF3.

Since both MdMYC2 and MdERF2 bind to the promoter of *MdACS1*, these two transcription factors might influence *MdACS1* expression by binding to each other's *cis*-elements in the *MdACS1* promoter. To investigate this possibility, we purified recombinant full-length MdMYC2 and MdERF2 proteins, as well as their binding domains (amino acids 500–600 for MdMYC2 and amino acids 190–250 for MdERF2), all of which had His tags, and performed EMSA analysis. Neither MdMYC2 nor MdERF2 interfered with the binding of the other to the *MdACS1* promoter (Supplemental Figures 5D and 5E).

JA Treatment Promotes the Transcriptional Regulation of Both *MdACS1* and *MdACO1* by MdMYC2, as Well as the MdMYC2-MdERF2 Interaction

To investigate whether JA promotes the transcription of *MdACS1* through transcriptional regulation of MdMYC2, we treated the abovementioned calli overexpressing MdMYC2-GFP with MeJA and conducted ChIP-PCR using an anti-GFP antibody. MdMYC2-GFP caused a greater enrichment of the *MdACS1* and *MdERF3* promoter DNA in MeJA-treated calli than in the untreated calli

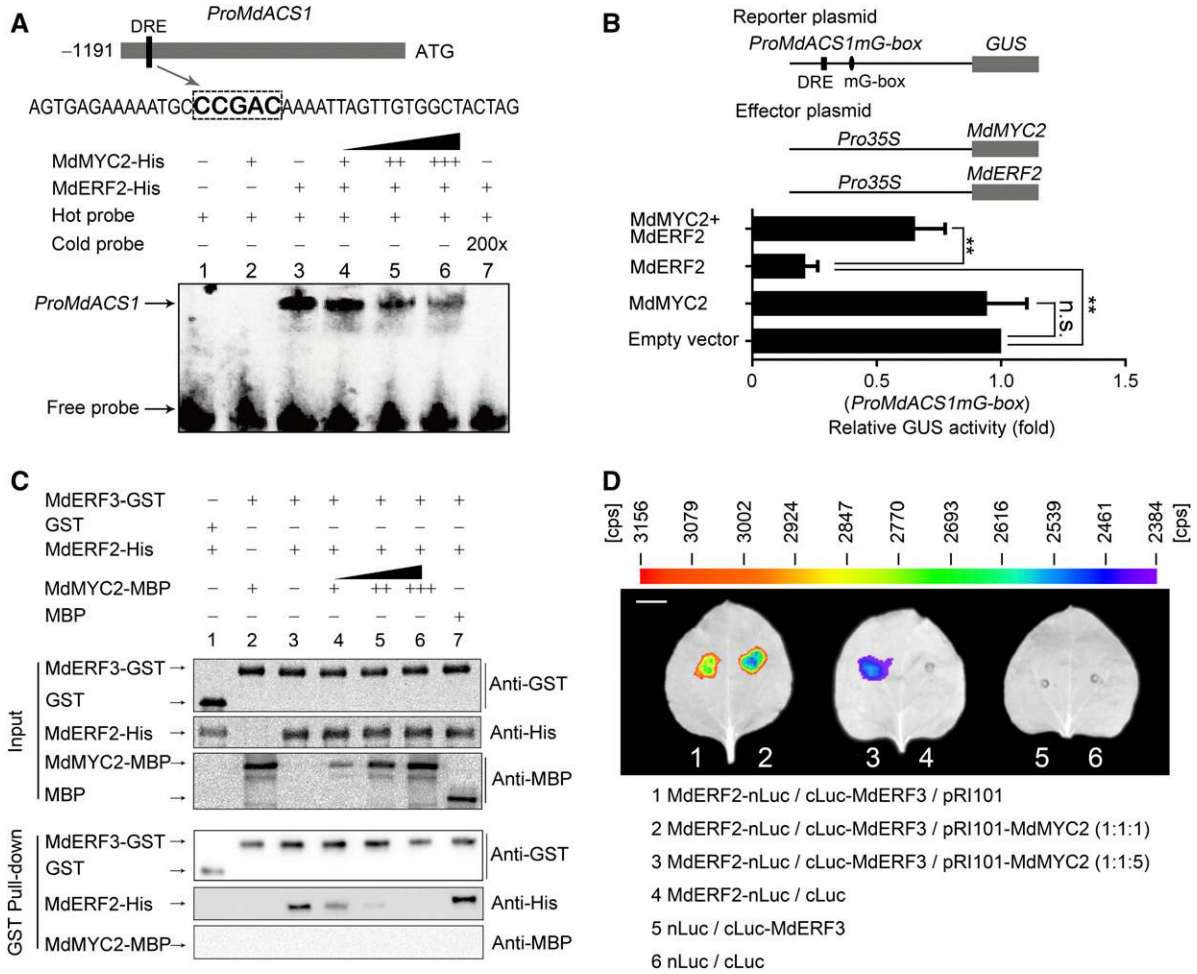

Figure 7. MdMYC2-MdERF2 Interaction Inhibits the Binding of MdERF2 to the *MdACS1* Promoter and Suppresses the MdERF2-MdERF3 Interaction.

(A) EMSA results showing that MdMYC2 did not bind to the DRE motif (−1040) in the *MdACS1* promoter (lane 2), but MdERF2 did bind to this motif (lane 3). MdMYC2 interfered with MdERF2 for binding to the *MdACS1* promoter (lanes 4–6). The hot probe was a biotin-labeled *MdACS1* promoter, while the cold probe was a nonlabeled competitive probe (200-fold higher concentration than that of the hot probe). His-tagged MdMYC2 (MdMYC2-His) and MdERF2 (MdERF2-His) were purified from *Escherichia coli* and used for the DNA binding assays. The sequence of the biotin-labeled probe is shown and the DRE motif is highlighted in bold.

(B) MdMYC2 or MdERF2 effector vectors alone or together with the reporter vector containing the *MdACS1* promoter, whose G-box motif was mutated (*ProMdACS1mG-box*) to ensure that MdMYC2 did not bind, were infiltrated into wild tobacco leaves to analyze the regulation of GUS activity. Error bars represent SE of measurements from three independent transfection experiments. Asterisks indicate significantly different values (**P < 0.01). n.s., no significant difference.

(C) The in vitro interaction between MdERF2 and MdERF3 is weakened by MdMYC2. MdMYC2-MBP and MdERF2-His were purified and incubated with immobilized MdERF3-GST. The immunoprecipitated fractions were visualized using an anti-His antibody. MdERF3-GST input is shown.

(D) A luciferase complementation imaging assay showing that MdMYC2 weakens the interaction between MdERF2 and MdERF3 in tobacco leaves. Agrobacterium strain EHA105 harboring different constructs was infiltrated into different wild tobacco leaf regions. Luciferase activities were recorded in these regions 3 d after infiltration. Bar = 1 cm; cps, signal counts per second.

(Figure 8A), indicating that JA promotes the binding of MdMYC2 to both *MdACS1*, thereby increasing its expression directly, and the *MdERF3* promoter, thereby increasing *MdACS1* expression indirectly. In addition, MdMYC2-GFP expression caused a greater enrichment of *MdACO1* promoter DNA in MeJA-treated calli than in untreated calli (Figure 8A), indicating that JA also promotes the binding of MdMYC2 to the *MdACO1* promoter, thereby directly increasing its expression.

We further investigated whether JA promotes *MdACS1* transcription by promoting the MdMYC2-MdERF2 interaction. First, we conducted a GUS transactivation assay in wild tobacco leaves following cotransformation with the *Pro35S:MdMYC2*, *Pro35S:MdERF2*, and *ProMdACS1mG-box:GUS* constructs, showing that MeJA treatment enhanced the activity of the *MdACS1* promoter when both MdMYC2 and MdERF2 were present (Figure 8B). Second, we coinfiltrated the MdERF2-nLuc, cLuc-MdERF3 and

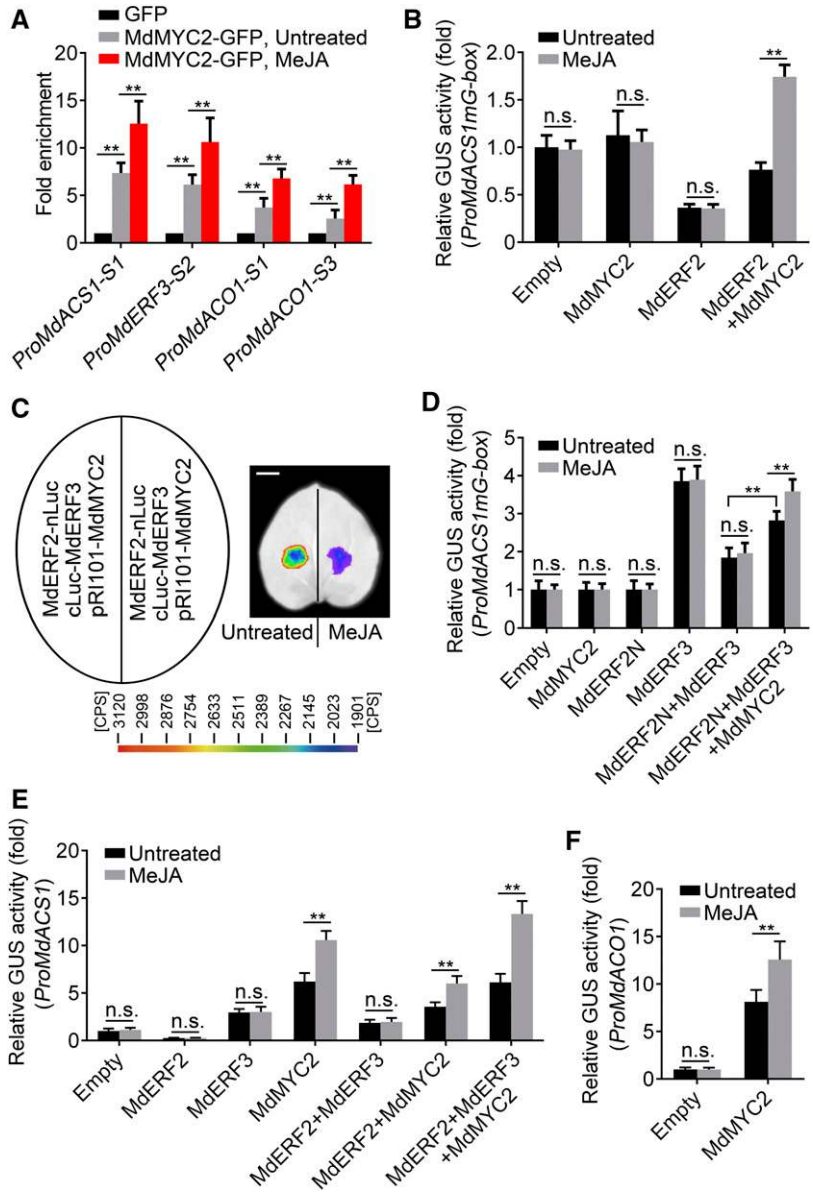

Figure 8. MeJA Treatment Increases the Binding of MdMYC2 to the Promoters of *MdACS1*, *MdACO1*, and *MdERF3* and Weakens the Interaction between MdERF2 and MdERF3.

(A) ChIP-PCR showing that JA treatment increases the binding of MdMYC2 to the promoters of *MdACS1*, *MdACO1*, and *MdERF3*. Cross-linked chromatin samples were extracted from MdMYC2-GFP-overexpressing fruit calli treated with or without MeJA and precipitated with an anti-GFP antibody. Eluted DNA was used to amplify the sequences neighboring the G-box by qPCR. *ProMdACS1-S1*, *ProMdACO1-S1/S3*, and *ProMdERF3-S2* refer to the promoter region of *MdACS1*, *MdACO1*, or *MdERF3* in Figures 3C, 3E, and Figure 5C, respectively.

(B) GUS activity assay showing that MeJA treatment inhibits the suppression by MdERF2 of the *MdACS1* promoter through the action of MdMYC2. MdMYC2 and MdERF2 effector vectors, together with the reporter vector containing the mutated *MdACS1* promoter (*ProMdACS1mG-box* as in Figure 7B), were infiltrated into wild tobacco leaves to analyze the regulation of GUS activity. Three independent transfection experiments were performed. Values represent means ± SE. Asterisks indicate significantly different values (**$P < 0.01$). n.s., no significant difference.

(C) A luciferase complementation imaging assay shows that JA treatment weakens the interaction between MdERF2 and MdERF3 in the presence of MdMYC2 in wild tobacco leaves. Wild tobacco leaves were infiltrated with Agrobacterium strain EHA105 harboring MdERF2-nLuc, cLuc-MdERF3, and pRI10-MdMYC2, followed by MeJA treatment, and luciferase activities were recorded in these regions 3 d after infiltration. Bar = 1 cm; cps, signal counts per second.

(D) GUS activity assay showing that MeJA treatment results in the activation of the *MdACS1* promoter through the MdMYC2-MdERF2 interaction. MdMYC2, MdERF2N, and MdERF3 effector vectors, together with the reporter vector containing the mutated *MdACS1* promoter (*ProMdACS1mG-box* as in Figure 7B), were infiltrated into wild tobacco leaves to analyze the regulation of GUS activity. MdERF2N is the N terminus of MdERF2, which interacts with

pRI101-MdMYC2 constructs into wild tobacco leaves, followed by MeJA treatment. The luminescence signal was weaker after MeJA treatment (Figure 8C). We then cotransformed the wild tobacco leaves with the *Pro35S:MdMYC2*/*Pro35S:MdERF2N*/*Pro35S:MdERF3* plasmids together with the *ProMdACS1mG-box:GUS* plasmid in a GUS transactivation assay. When *Pro35S:MdMYC2*, *Pro35S:MdERF2N* and *Pro35S:MdERF3* were co-transformed together with *ProMdACS1mG-box:GUS*, the GUS activity level was significantly higher than that after the transformation of *Pro35S:MdERF2N* and *Pro35S:MdERF3* together with *ProMdACS1mG-box:GUS*, especially under MeJA treatment (Figure 8D). These results indicate that MeJA treatment inhibits the binding of MdERF2 to MdERF3 by promoting the MdMYC2-MdERF2 interaction, resulting in more MdERF3 being available to activate *MdACS1* expression.

Finally, we investigated the effects of JA on *MdACS1* and *MdACO1* expression using a GUS transactivation assay in wild tobacco leaves. When MdMYC2, MdERF2, and MdERF3 were coinfiltrated with the *MdACS1* promoter in wild tobacco leaves, the activity of the *MdACS1* promoter was significantly enhanced by MeJA treatment (Figure 8E). Similarly, when MdMYC2 was coinfiltrated with the promoter of *MdACO1*, the activity of the *MdACO1* promoter was significantly enhanced by MeJA treatment (Figure 8F).

MdMYC2 Is Required for JA-Induced Promotion of Ethylene Production in Apple Fruit

The generation and testing of transgenic apple fruit are technically and experimentally challenging due to the long juvenile period (Kotoda et al., 2006). We therefore used a transient expression assay involving Agrobacterium infiltration to silence *MdMYC2* expression in apple fruit to further confirm the role of *MdMYC2* in JA-induced ethylene biosynthesis. A partial CDS of *MdMYC2* was ligated into the pTRV virus vector, and the resulting construct was used for fruit infiltration. Fruits were harvested at 14 d after infiltration and fruit infiltrated with the empty pTRV vector were used as a control. In the *MdMYC2*-suppressed apple fruit (MdMYC2-AN), MdMYC2 transcript and protein levels were significantly reduced (Figures 9A and 9B). These fruits were treated with MeJA and stored at room temperature for 20 d (Figure 9C). After MeJA treatment, MdMYC2-AN fruits showed significantly lower *MdACS1* and *MdACO1* expression compared with the control fruits (Figures 9D and 9E), and the pattern of ethylene production was the same as the pattern of expression of both *MdACS1* and *MdACO1* (Figure 9G). These findings indicate that MdMYC2 is required for JA-promoted ethylene production in apple fruit.

DISCUSSION

JA has been implicated in promoting ethylene production in several species, including apple (Saniewski and Czapski, 1985; Saniewski et al., 1987; Fan et al., 1997; Kondo et al., 2009; Khan and Singh, 2015; Lalel et al., 2015). For example, JA treatment markedly increases the expression of *MdACS1* and *MdACO1*, as well as ethylene production, in apple fruit during ripening (Fan et al., 1997, 1998; Kondo et al., 2009). However, the molecular mechanism by which JA promotes ethylene production and the expression of ethylene biosynthetic genes during fruit ripening have been unclear. In this study, we found that the expression of *MdMYC2*, which encodes an important transcription factor in the JA signaling pathway, was markedly increased in apple fruit treated with MeJA; moreover, JA promotes ethylene production through the regulation of *MdACS1* and *MdACO1* transcription by MdMYC2.

JA-Activated MdMYC2 Directly Enhances the Expression of Ethylene Biosynthetic Genes in Apple Fruit

Apple is a typical climacteric fruit that produces large amounts of ethylene during ripening (Kende, 1993; Oraguzie et al., 2004). The importance of ACS and ACO in ethylene biosynthesis is well established (Sunako et al., 1999; Giovannoni, 2004; Oraguzie et al., 2004; Barry and Giovannoni, 2007; Wang et al., 2009; Tan et al., 2013; Li et al., 2015), and silencing of *MdACS1* or *MdACO1* in apple fruit results in a substantial reduction in ethylene production (Dandekari et al., 2004; Schaffer et al., 2007). We observed that the expression of both *MdACS1* and *MdACO1* was promoted by MeJA treatment in mature apple fruit (Figure 1). Since there are four other *ACS* genes (*MdACS3a*, *4*, *5*, and *6*) in the apple genome (Kim et al., 1992; Sunako et al., 2000; Wang et al., 2009; Li et al., 2015), we also investigated their expression in apple fruit treated with MeJA. None of these genes was induced by MeJA treatment (Supplemental Figure 9), indicating that these *MdACS* genes are not involved in JA-induced ethylene biosynthesis. *MdACO1* is the only *ACO* gene that is highly expressed in apple fruit (Wakasa et al., 2006; Wiersma et al., 2007) and is induced by JA treatment (Kondo et al., 2009). Accordingly, we focused only on *MdACS1* and *MdACO1* in this study.

Figure 8. (continued).

both MdMYC2 and MdERF3 but does not bind the *MdACS1* promoter. Three independent transfection experiments were performed. Values represent means ± SE. Asterisks indicate significantly different values (**P < 0.01). n.s., no significant difference.

(E) GUS activity assay showing that MeJA treatment results in the activation of the *MdACS1* promoter through the action of MdMYC2. MdMYC2, MdERF2, and MdERF3 effector vectors, together with the reporter vector containing the *MdACS1* promoter, were infiltrated into wild tobacco leaves to analyze the regulation of GUS activity. Three independent transfection experiments were performed. Values represent means ± SE. Asterisks indicate significantly different values (**P < 0.01). n.s., no significant difference.

(F) GUS activity assay showing that MeJA treatment results in the activation of the *MdACO1* promoter through the action of MdMYC2. The MdMYC2 effector vector and the reporter vector containing the *MdACO1* promoter were infiltrated into wild tobacco leaves to analyze the regulation of GUS activity. Three independent transfection experiments were performed. Values represent means ± SE. Asterisks indicate significantly different values (**P < 0.01). n.s., no significant difference.

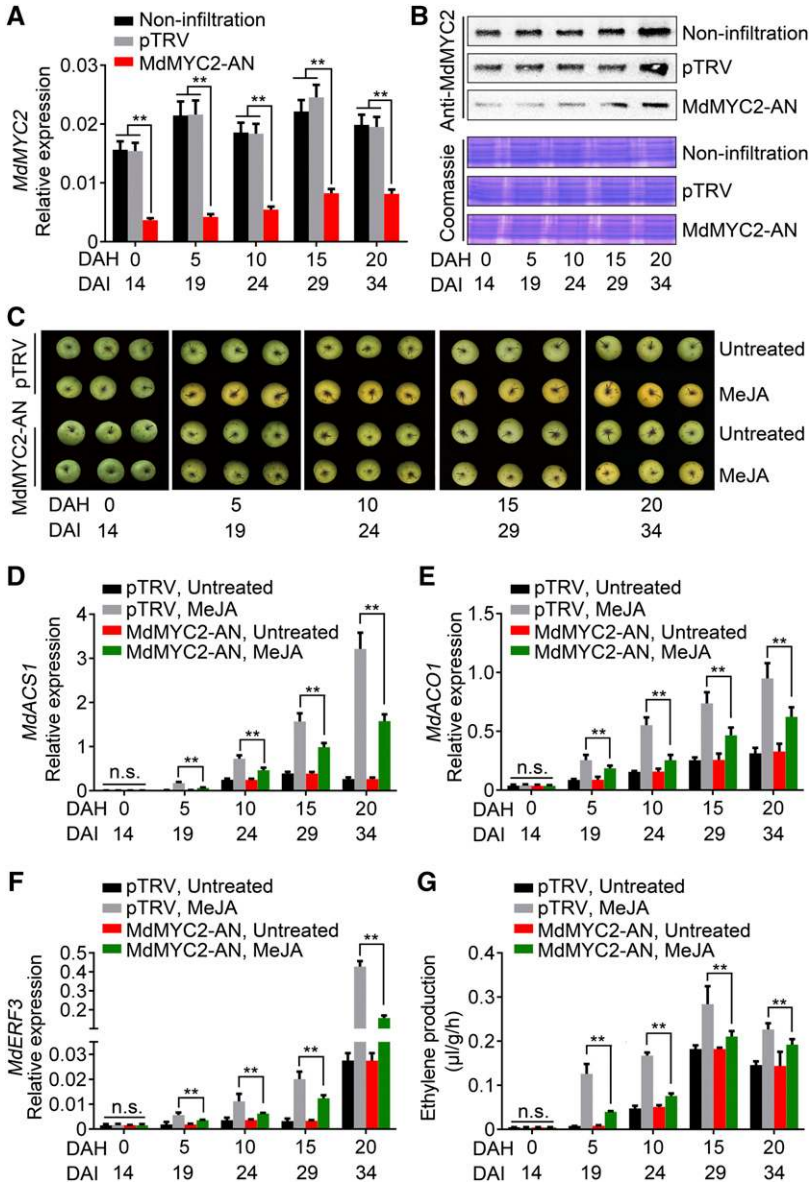

Figure 9. *MdMYC2* Is Essential for JA-Induced Ethylene Biosynthesis in Apple Fruit.

(A) and **(B)** *MdMYC2* was silenced in apple fruits (MdMYC2-AN) by Agrobacterium-mediated transient transformation. MdMYC2-AN fruits were harvested 14 d after infiltration and stored at room temperature for 20 d. *MdMYC2* expression was investigated by qRT-PCR **(A)** and immunoblot analysis **(B)**. Noninfiltrated fruits or fruits infiltrated with an empty pTRV vector were used as controls. A Coomassie-stained SDS-PAGE gel (Coomassie) was used to confirm equal sample loading.

(C) to **(G)** MdMYC2-AN fruits were treated with MeJA immediately after harvest and stored at room temperature for 20 d **(C)**. The expression levels of *MdACS1* **(D)**, *MdACO1* **(E)**, and *MdERF3* **(F)** were investigated by qRT-PCR. Ethylene production was measured **(G)**. Untreated, fruits not receiving MeJA treatment; MeJA, fruits receiving MeJA treatment; DAI, days after infiltration. For qRT-PCR, three biological replicates were performed as described in the legend of Figure 1. Values represent means ± SE. Statistical significance was determined using a Student's *t* test (**$P < 0.01$). n.s., no significant difference.

We found that MeJA treatment did not promote *MdACS1* expression or ethylene production in apple fruits in which *MdACS1* expression had not initiated (Figures 1C and 1D; Supplemental Figures 1A and 1C). In fruits treated with 1-MCP, the expression of *MdACS1* was blocked, and the application of MeJA to these fruits did not induce *MdACS1* expression (Figure 1G) or promote ethylene production (Figure 1H). By contrast, in fruits in which *MdACS1* expression had initiated, MeJA significantly promoted *MdACS1* expression (Figures 1C and 1G) and ethylene production (Figures 1D and 1H). These results suggest that JA can promote ethylene biosynthesis in apple fruit only if *MdACS1* is already being expressed. Moreover, we demonstrated that MdMYC2

bound to the promoters of both *MdACS1* and *MdACO1* and induced their expression (Figure 3), with JA enhancing both the binding and expression of the genes (Figure 8). These results suggest that JA-activated MdMYC2 promotes both the biosynthesis of ACC by inducing *MdACS1* expression and the oxidation of ACC to ethylene by inducing *MdACO1* expression. We therefore conclude that JA-promoted ethylene biosynthesis in fruit ripening is dependent on the expression of ethylene biosynthetic genes.

JA-Activated MdMYC2 Enhances *MdACS1* Transcription through MdERF3

We previously reported that MdERF3 promotes the transcription of *MdACS1* by binding to its promoter (Li et al., 2016). In this study, we found that MdMYC2 bound to the *MdERF3* promoter in vivo (Figure 5C) and that MeJA treatment enhanced this binding (Figure 8A). Moreover, MdMYC2 induced the transcription of *MdERF3* (Figure 5D). We conclude that JA promotes the binding of MdMYC2 to the *MdERF3* promoter, thereby promoting the transcription of *MdERF3*, which in turn promotes *MdACS1* transcription and ethylene production.

Since we noted that an ERF binding site (DRE motif) was present in the *MdMYC2* promoter, we investigated whether the MdERF3 transcription factor could bind to the *MdMYC2* promoter. A ChIP-PCR assay showed that MdERF3 bound to the *MdMYC2* promoter region containing the DRE motif (Supplemental Figure 10), indicating that MdMYC2 and MdERF3 can mutually promote their transcription, thereby strengthening the regulation of *MdACS1* transcription in response to JA.

Han et al. (2016) reported that MaERF11 can bind to the promoter of *MaACO1* and suppresses its expression in banana, but we did not identify an ERF binding site in the *MdACO1* promoter (2000 bp), and MdERF3 was not able to bind the *MdACO1* promoter based on ChIP-PCR analysis (Supplemental Figure 6). This suggests that the mechanism by which ERF proteins act on *ACO* genes may differ between species, and we conclude that MdMYC2 is not able to regulate the transcription of *MdACO1* through MdERF3.

JA-Activated MdMYC2-MdERF2 Interaction Enhances the Transcription of *MdACS1*

We obtained evidence for an interaction between MdMYC2 and MdERF2 (Figure 6; Supplemental Figure 7). One effect of the MdMYC2-MdERF2 interaction on *MdACS1* expression might be on the binding to the *MdACS1* promoter. MdERF2 is a transcriptional repressor that binds to the *MdACS1* promoter and suppresses its expression (Li et al., 2016). In this study, we found that the presence of MdMYC2 inhibited the binding of MdERF2 to the *MdACS1* promoter and enhanced its activity (Figure 7), with MeJA treatment strengthening this effect (Figure 8B). These results suggest that JA enhances the MdMYC2-MdERF2 interaction to suppress the binding of MdERF2 to the *MdACS1* promoter, thereby enhancing *MdACS1* transcription.

We observed that the MdMYC2-MdERF2 interaction inhibited the binding of MdMYC2 to the promoters of both *MdACS1* and *MdACO1* in EMSA analyses (Supplemental Figures 8A and 8C) and reduced the regulation of their expression by MdMYC2 in GUS transactivation assays (Supplemental Figures 8B and 8D). However, *MdERF2* expression was not altered by MeJA treatment in apple fruit (Figure 4B), indicating that in response to MeJA treatment, MdERF2 does not influence the regulation of its downstream genes by MdMYC2. We therefore conclude that the MdMYC2-MdERF2 interaction does not influence the promotion of *MdACS1* and *MdACO1* expression by MdMYC2 in apple fruit in response to JA.

Another effect of the MdMYC2-MdERF2 interaction on *MdACS1* expression might be to influence the MdERF2-MdERF3 interaction, thereby affecting *MdACS1* expression: We previously showed that the N terminus of MdERF2 interacts with the binding domain of MdERF3 and inhibits the binding of MdERF3 to the *MdACS1* promoter, as well as suppressing *MdACS1* transcription (Li et al., 2016). In this study, we found that MdMYC2 interacted with the N terminus of MdERF2 (Figure 6). The MdMYC2-MdERF2 interaction inhibited the binding of MdERF2 to MdERF3 (Figure 7), and MeJA treatment strengthened this inhibition (Figure 8C). These results suggest that the JA-activated MdMYC2-MdERF2 interaction inhibits the binding of MdERF2 to MdERF3, which in turn leads to higher levels of free MdERF3. In addition, our previous study revealed that MdERF2 and MdERF3 bind to the same DRE motif in the *MdACS1* promoter, although MdERF2 suppresses *MdACS1* expression, while MdERF3 induces its expression (Li et al., 2016). It is therefore possible that MdERF2 and MdERF3 compete with each other for binding to the *MdACS1* promoter. To address this possibility, we performed EMSA analysis with purified MdERF2 and MdERF3 proteins. Increasing amounts of MdERF2 inhibited the binding of MdERF3 to the *MdACS1* promoter (Supplemental Figure 11A), and increasing amounts of MdERF3 inhibited the binding of MdERF2 to the *MdACS1* promoter (Supplemental Figure 11B). We then conducted a GUS transactivation assay to determine their combined influence on *MdACS1* expression. Increasing amounts of MdERF2 reduced the activation of the *MdACS1* promoter by MdERF3 (Supplemental Figure 11C), while increasing amounts of MdERF3 inhibited its suppression (Supplemental Figure 11D). These results indicate that MdERF2 and MdERF3 compete with each other for binding to the *MdACS1* promoter to regulate its expression. Moreover, the coinfiltration of MdMYC2, MdERF2, and MdERF3 significantly enhanced *MdACS1* expression under MeJA treatment in GUS transactivation assays (Figures 8D and 8E). These results indicate that the increased levels of MdERF3 resulting from the MdMYC2-MdERF2 interaction further promote *MdACS1* transcription.

Collectively, we conclude that the JA-activated MdMYC2-MdERF2 interaction not only prevents MdERF2 from binding to the *MdACS1* promoter, resulting in more binding for MdERF3, but it also prevents MdERF2 from interacting with MdERF3, resulting in the greater availability of MdERF3 for binding to the *MdACS1* promoter. Both modes of action could lead to enhanced expression of *MdACS1*.

MdMYC2 Is Essential for JA-Promoted Ethylene Production in Apple Fruit

We further investigated whether MdMYC2 is required for JA to promote ethylene production in apple fruit. Due to the long juvenile

period of transgenic apple plants, we used a transient expression assay to silence *MdMYC2* expression in apple fruit by Agrobacterium infiltration, a widely used method for studying gene function (Jia et al., 2011; Wang et al., 2013; Han et al., 2015; Li et al., 2016). *MdMYC2*-suppressed apple fruit (MdMYC2-AN) showed slower ripening than control fruits after MeJA treatment (Figure 9C), as well as significantly lower *MdACS1* and *MdACO1* expression (Figures 9D and 9E) and ethylene production (Figure 9G). These results support the conclusion that JA promotes ethylene biosynthesis in apple fruit through the regulation of MdERFs and ethylene biosynthetic genes by MdMYC2.

Although JA-promoted ethylene production has been reported in various fruit species (Saniewski and Czapski, 1985; Saniewski et al., 1987; Fan et al., 1997, 1998; Kondo et al., 2009; Khan and Singh, 2015; Lalel et al., 2015), most of these studies only focused on the changes in *ACS* or *ACO* expression and ethylene production. In contrast, our work links JA and ethylene biosynthesis by shedding light on the regulation of *MdERFs*, *MdACS1*, and *MdACO1* by MdMYC2.

In apple calli treated with MeJA, both *MdACS1* and *MdACO1* showed significantly reduced expression levels in *MdMYC2*-suppressed calli compared with the control, while in untreated calli, *MdACS1* and *MdACO1* showed the same expression levels in *MdMYC2*-suppressed calli as in the control (Figure 2C), although MdMYC2 was shown to bind the promoters of *MdACS1* and *MdACO1* in vivo (Figure 3). A similar phenomenon was observed for JA-promoted chlorophyll degradation in Arabidopsis (Zhu et al., 2015). In that study, AtMYC2 bound to the promoter of pheophorbide *a* oxygenase (*PAO*) gene, a key gene in chlorophyll degradation. Following JA treatment, *AtPAO* expression was enhanced in control plants but was not altered in *AtMYC2*-silenced plants, whereas in the absence of JA treatment, *AtPAO* expression did not significantly differ between the control and *AtMYC2*-silenced plants (Zhu et al., 2015). These results suggest that MYC2 cannot activate the transcription of downstream genes without JA. Since JAZ acts as a transcriptional repressor of MYC2 by interacting with it when JA is unavailable (Kazan and Manners, 2013), we propose that MdMYC2 is immobilized by JAZ in untreated calli, so that MdMYC2 is not able to promote the expression of *MdACS1* and *MdACO1*. Moreover, MdMYC2 bound to the promoters of both *MdACS1* and *MdACO1* even without MeJA treatment (Figure 3). A similar result was observed for JA-regulated hook development in Arabidopsis, in which AtMYC2 binds to the promoter of an *F-box* gene without JA

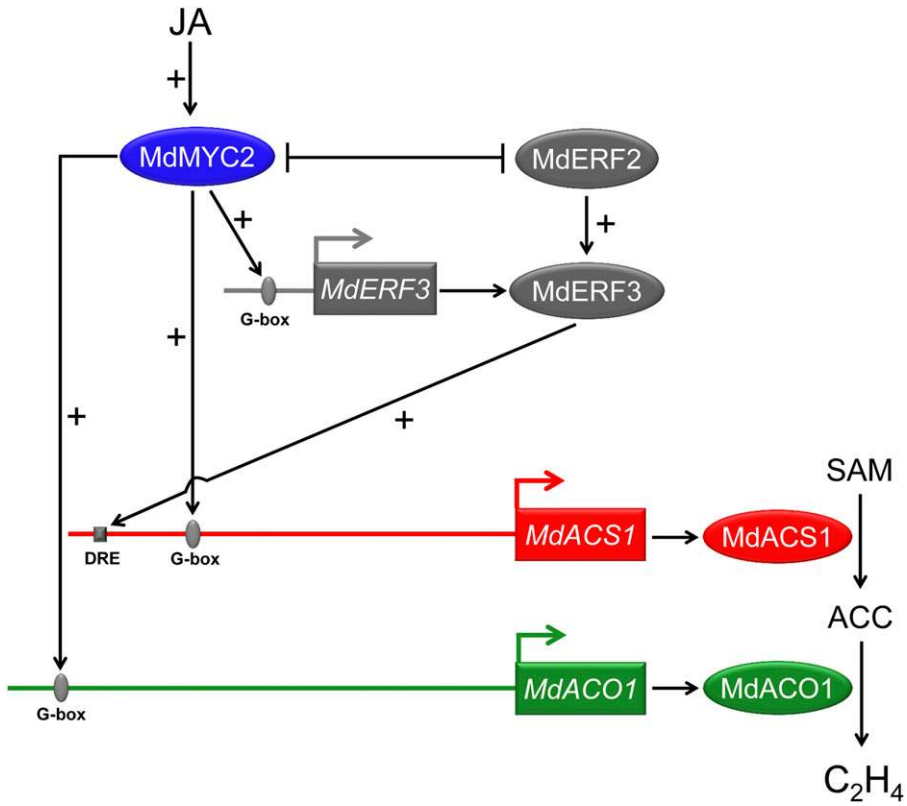

Figure 10. Model Showing the Promotion of Ethylene Biosynthesis by JA-Induced MdMYC2 through the Regulation of MdERFs and Ethylene Biosynthetic Genes.

MdMYC2 binds to the promoters of both *MdACS1* and *MdACO1* and enhances their action. MdMYC2 promotes the activity of MdERF3, which binds to the *MdACS1* promoter and activates *MdACS1* transcription. In addition, MdMYC2 and MdERF2 directly interact, inhibiting the suppression by MdERF2 of the *MdACS1* promoter and preventing MdERF2 from binding to MdERF3, leading to higher levels of free MdERF3 for transactivation of *MdACS1*. Through these three mechanisms, MdMYC2 promotes the transcription of *MdACS1* and *MdACO1* and ethylene biosynthesis in response to JA during apple fruit ripening. "+", promotion; solid arrow, direct regulation; G-box, MYC binding site; SAM, *S*-adenosyl methionine; C_2H_4, ethylene.

treatment (Zhang et al., 2014). Perhaps the JAZ-MYC2 repressor complex constitutively binds to its target promoters even when JA is unavailable. Future work will focus on the interaction between JAZ and MdMYC2 or other transcription factors to elucidate their roles in JA-induced ethylene production in apple fruit.

Taken together, our data indicate that JA-activated MdMYC2 promotes ethylene biosynthesis in apple through three mechanisms: (1) enhancing the transcription of both *MdACS1* and *MdACO1* by binding to their promoters; (2) enhancing the transcription of *MdERF3* by binding to its promoter, which in turn promotes the transcription of *MdACS1*; and (3) interacting with MdERF2, which prevents MdERF2 from binding to the *MdACS1* promoter and from interacting with MdERF3, resulting in more MdERF3 being available for binding to the *MdACS1* promoter and a consequent increase in *MdACS1* transcription (Figure 10).

METHODS

Plant Material and Treatments

Malus domestica cv GD fruits were sampled from mature trees growing in the experimental farm of the Liaoning Pomology Institute (Xiongyue, China). GD fruits were harvested at 110, 125, and 140 DAFB and immediately transferred to the laboratory. Fruits harvested at 140 DAFB were divided into four groups (30 fruits per group). The first group was not treated. The second group was treated with MeJA (Sigma-Aldrich). MeJA was dissolved in 100% ethanol, diluted to 100 μM with water, and sprayed onto the surface of the fruits. The third group was treated with 1-MCP (an ethylene antagonist) as described (Tan et al., 2013). The fourth group was treated with 1-MCP for 12 h, followed by MeJA treatment. These four groups of fruit were stored at room temperature (24°C) for 20 d, with sampling every 5 d during the storage period. Ethylene production was measured at each sampling time as previously described (Li et al., 2014). Fruits harvested at 110 or 125 DAFB were divided into two groups. One group was treated with MeJA as described above, and the other group was used as the control. The sampling regime and procedure for measuring ethylene were as described above.

Apple fruit calli (cv Orin) and wild tobacco (*Nicotiana benthamiana*) plants were used for *Agrobacterium tumefaciens* infection; their growing conditions were as described (Li et al., 2016). For MeJA treatment of calli, 100 μM MeJA was added to the medium.

RNA Extraction, cDNA Synthesis, and qRT-PCR

Total RNA extraction and cDNA synthesis were performed as previously described (Li et al., 2015). The first-strand cDNA was synthesized from 1 μg of total RNA using an M-MLV RTase cDNA Synthesis Kit (catalog no. D6130; TaKaRa). For standard PCR, the total volume of PCR mixture was 20 μL, containing 10 μL of 2×EX Taq Mix (catalog no. RR902A; TaKaRa), 1 μL of forward primer and 1 μL of reverse primer (0.5 μM for each), and 1 μL of template cDNA. The final volume was brought to 20 μL by adding 7 μL of water. The thermal cycling conditions were 5 min at 95°C; 30 or 35 cycles of 30 s at 95°C, 30 s at 55°C and 1 min at 72°C; and a final extension of 5 min at 72°C. Five microliters of each PCR product was separated on a 1% agarose gel and photographed with a GelDoc XR System (Bio-Rad). qRT-PCR was conducted on an Applied Biosystems 7500 Real-Time PCR System as previously described (Tan et al., 2013) in 20 μL of reactions containing 1 μL of cDNA, 0.5 μM of the forward and reverse primer, and 1× SYBR green master mix (catalog no. 04707516001; Roche). The reaction program had an initial denaturation step of 5 min at 95°C, 40 cycles of amplification using 15 s at 95°C, 30 s at 55°C, and 30 s at 72°C, and a dissociation stage of 15 s at 95°C, 1 min at 60°C, and 30 s at 95°C. Fruits sampled at each sampling point were divided into three groups (two fruits per group). The fruit flesh in each group was evenly mixed for RNA extraction. RNA extracted from each group was used as one biological replicate in qRT-PCR. A total of three biological replicates were conducted. For calli samples, each successfully infected line was grown on three separated plates containing solid medium. Those calli grown on each plate were used as one biological replicate. All primers used to detect gene expression are listed in Supplemental Data Set 1.

Immunoblot Analysis

Protein extraction and immunoblot analysis were performed as by Li et al. (2015). Purified MdMYC2-His proteins were used for raising an anti-rabbit antibody. Anti-His (1 mg/mL; catalog no. CW0286; CWbiotech), anti-GST (1 mg/mL; catalog no. CW0084; CWbiotech), anti-GFP (1 mg/mL; catalog no. HT801; Transgen Biotech), anti-MdACS1, anti-MdERF2 (Li et al., 2016), and anti-MdMYC2 antibodies were diluted 1:1000 with TBST buffer (Li et al., 2016) and incubated with nitrocellulose membranes (Solarbio). The secondary antibody (goat anti-mouse or anti-rabbit horseradish peroxidase-conjugated, 1 mg/mL; catalog no. CW0102 or CW0103; CWbiotech) was diluted 1:3000 with TBST buffer.

Protein Expression and Purification

The purification of MdERF2-His and MdERF3-GST was performed as previously described (Li et al., 2016). The CDS regions of *MdERF2N*, *MdERF2D*, and *MdERF2C* were cloned downstream from the GST encoding sequence in the pGEX4T-1 vector (GE Healthcare) in order to generate GST fusion proteins. The CDS regions of *MdMYC2*, *MdMYC2N* (1–344 amino acids), *MdMYC2D* (500–600 amino acids), *MdERF2*, *MdERF2D* (190–250 amino acids), *MdERF3*, and *MdERF3D* (140–200 amino acids) were cloned into the pEASY-E1 vector (Transgen Biotech) to express His fusion proteins. The CDS of *MdMYC2* was cloned into the pMAL-C2X vector (New England Biolabs) to generate MBP fusion proteins. The transformation of the resulting plasmids into *Escherichia coli* BL21 (DE3), and the induction of the target proteins was performed as previously described (Li et al., 2016). The isopropyl β-D-1-thiogalactopyranoside concentration for inducing protein expression was 0.5 mM, and the purification of the GST- or His-tagged fusion proteins was performed as previously described (Li et al., 2016). The purification of the MBP-tagged fusion protein was performed as by Yuan et al. (2014). All primers used are listed in Supplemental Data Set 1.

Y2H Assay

The ligation of full-length *MdERF2*, *MdERF2N*, *MdERF2D*, and *MdERF2C* into the activation domain (AD) vector (pGADT7; Clontech) was performed as previously described (Li et al., 2016). The CDS regions of *MdERF1* and *MdERF3* were ligated into the pGADT7 vector using the *Eco*RI and *Bam*HI restriction sites. The full-length *MdMYC2* CDS, *MdMYC2N* (1–344 amino acids) and *MdMYC2C* (345–688 amino acids) were ligated into the pGBKT7 (Clontech) binding domain (BD) vector using the *Nde*I and *Bam*HI sites. The primers used are shown in Supplemental Data Set 1. BD and AD vectors were cotransformed into the Y2HGold yeast strain. The detection of interactions between two proteins was conducted using the Matchmaker Gold Yeast Two-Hybrid Library Screening System kit (catalog no. 630489; Clontech).

Pull-Down Assay

To confirm the interaction between MdMYC2N and MdERF2N, 5 μg of purified His fusion protein (MdMYC2N) was bound to Ni-NTA His binding resin (Novagen). GST fusion proteins containing MdERF2N, MdERF2D, or MdERF2C were added and incubated for 1 h at 4°C with the subsequent

steps performed as previously described (Li et al., 2016). GST protein was used as the negative control.

For the competitive pull-down assays, 2 μg of in vitro-expressed and purified GST fusion proteins (MdERF3-GST and GST) were incubated with Glutathione Sepharose 4B (GE Healthcare) in pull-down buffer (50 mM Tris-Cl, pH 8.0, 150 mM NaCl, 10% glycerol, 0.5 mM EDTA, 0.1% Triton X-100, 5 mM mercaptoethanol, and 1× protease inhibitor cocktail) at 4°C for 4 h. MdERF2-His combined with MdMYC2-MBP (2, 6, or 12 μg) or MBP protein (negative control) was incubated with immobilized MdERF3-GST (2 μg) or GST (2 μg; negative control) at 4°C for 4 h. Precipitated Sepharose beads were washed three times with pull-down buffer by centrifugation (2000*g*, 1 min) and collected by centrifugation (2000*g*, 1 min). Proteins bound to the beads were resuspended in protein extraction buffer and separated by SDS-PAGE. Proteins were detected by immunoblot with anti-GST, anti-His, or anti-MBP (1 mg/mL; catalog no. CW0288; CWbiotech) antibodies as previously described.

Co-IP Assay

For the co-IP assay, the CDS of *MdMYC2* was cloned into the *Kpn*I and *Bam*HI sites downstream of the GFP sequence and the CaMV 35S promoter in the pRI101 vector (TaKaRa). The recombinant pRI101-GFP-MdMYC2 construct was introduced into apple calli as previously described (Xie et al., 2012), and the transgenic calli were used for co-IP analysis. The procedures for co-IP were as previously described (Li et al., 2016). A Pierce coimmunoprecipitation kit (catalog no. 26149; Thermo Scientific) was used to immunoprecipitate GFP-MdMYC2 using an anti-GFP antibody (1 mg/mL; catalog no. HT801; Transgen Biotech). The precipitate was analyzed by immunoblot analysis with the anti-ERF2 antibody. Untransformed calli were used as the negative control.

Y1H Assay

The CDS of *MdMYC2* was ligated into the pGADT7 vector (Clontech). Each *MdACS1* or *MdERF3* promoter fragment was ligated into the pAbAi vector (Clontech). All primers used are listed in Supplemental Data Set 1. The Y1H assay was conducted as previously described (Li et al., 2016).

EMSA

Proteins were purified as described above. Oligonucleotide probes were synthesized and labeled with biotin (Sangon Biotech). The 3′ biotin end-labeled double-stranded DNA probes were prepared by annealing complementary oligonucleotides, in which the oligonucleotides were heated at 95°C for 5 min, then at 72°C for 20 min, and immediately left to cool to room temperature before use. The biotin-labeled *MdACS1* promoter and *MdERF3* promoter sequences were as shown in Figures 3 and 5. EMSA was performed as previously described (Li et al., 2016).

ChIP-PCR Analysis

The recombinant pRI101-GFP-MdMYC2 construct or pRI101-Myc-MdERF2/3 constructs were transformed into apple calli as described above, and the ChIP assays were performed as previously described (Li et al., 2016) with an anti-GFP antibody (Transgen Biotech). The amount of immunoprecipitated chromatin was determined by qPCR as previously described (Li et al., 2016). Each ChIP assay was repeated three times and the enriched DNA fragments in each ChIP sample were used as one biological replicate for qPCR. One microliter of immunoprecipitated chromatin was used as template for the qPCR analysis. Four regions of the *MdACS1* promoter, eight regions of the *MdACO1* promoter, and five regions of the *MdERF3* promoter were analyzed to assess their enrichment. Primers used are listed in Supplemental Data Set 1.

GUS Analysis

Reporter constructs containing the promoter sequences of *MdACS1* (1191 bp upstream of the start ATG), *MdACO1* (1240 bp upstream of the start ATG), or *MdERF3* (1158 bp upstream of the start ATG) were prepared as previously described (Li et al., 2016). A mutation was introduced into the G-box motif of the *MdACS1* promoter using a Fast Mutagenesis System kit (Transgen Biotech). The CDS of *MdMYC2*, *MdERF2*, *MdERF2N*, *MdERF2D*, or *MdERF3D* was introduced into the pRI101 vector using restriction enzyme sites (*Kpn*I and *Bam*HI for MdMYC2; *Nde*I and *Eco*RI for MdERF2) to generate the effector constructs. The transfection of reporter and effector constructs into wild tobacco leaves and measurements of GUS activity were performed as previously described (Li et al., 2016). MeJA treatment (10 μM) was applied to wild tobacco leaves 3 h before imaging. The primers are listed in Supplemental Data Set 1.

Firefly Luciferase Complementation Imaging Assay

The CDS of *MdERF2* and *MdERF3* were inserted into the pCAMBIA1300-nLuc vector (Chen et al., 2008) using the *Sal*I and *Bam*HI or *Kpn*I and *Sal*I restriction enzyme sites, respectively. MdMYC2 was inserted into the pRI101 vector using the *Kpn*I and *Bam*HI sites. Agrobacterium strain EHA105 carrying the indicated constructs was cultured to OD_{600} 0.5, combined with different volumes of the adjusted culture for specific groups, as shown in Figure 7D, and incubated at room temperature for 3 h before being infiltrated into wild tobacco leaves. Luciferase activity was detected 3 d after infiltration using the NightSHADE LB 985 imaging system (Berthold Technologies). Thirty minutes before detection, 0.2 mM luciferin (Promega) was infiltrated into the same positions at which Agrobacterium was infiltrated. MeJA treatment (10 μM) was applied to Agrobacterium-infiltrated wild tobacco leaves 3 h before imaging.

Agrobacterium Infiltration

To silence *MdMYC2* expression in apple fruit calli, a partial *MdMYC2* CDS (286–1349 bp) was ligated into the pRI101 vector in the reverse direction to generate the antisense pRI101-MdMYC2-AN construct. The recombinant plasmids were transformed into Agrobacterium strain EHA105. The preparation of infection suspension and silencing of *MdMYC2* expression in apple calli were performed as previously described (Xie et al., 2012). To silence *MdMYC2* expression in apple fruit, a partial *MdMYC2* CDS (1250–1750 bp) was ligated into the pTRV vector (The Samuel Roberts Noble Foundation; http://www.noble.org/). The recombinant plasmid was transformed into Agrobacterium strain EHA105. The preparation of infection suspension and silencing of *MdMYC2* expression in apple fruit were performed as previously described (Li et al., 2016).

Accession Numbers

Sequence data from this article can be found in the Genome Database for Rosaceae (https://www.rosaceae.org/) or GenBank/EMBL libraries under accession numbers *MdMYC2* (MDP0000136498), *MdMYC2-like 1* (MDP0000242554), *MdMYC2-like 2* (MDP0000900024), *MdMYC2-like 3* (MDP0000442310), *MdERF1* (AB288347), *MdERF2* (AB288348), *MdERF3* (XM_008339725), *MdACS1* (U89156), *MdACS3a* (AB243060), *MdACS4* (XM_008366591), *MdACS5* (AB034992), *MdACS6* (MDP0000133334), *MdACO1* (AF030859), and *Actin* (EB136338).

Supplemental Data

Supplemental Figure 1. *MdACS1* and *MdACO1* Expression and Ethylene Production in Apple Fruits Harvested at 110 DAFB.

Supplemental Figure 2. Expression of *MdMYC* Genes in Apple Fruit.

Supplemental Figure 3. Sequence Alignment of *MdMYC2* with Its Homologs from *Arabidopsis thaliana* and *Nicotiana tabacum*.

Supplemental Figure 4. ChIP-PCR Shows That MdMYC2 Does Not Bind to the *MdERF1* or *MdERF2* Promoters.

Supplemental Figure 5. Interference between MdMYC2 and MdERF3 or MdERF2 in Binding to the *MdACS1* Promoter.

Supplemental Figure 6. ChIP-PCR Analysis Showing that neither MdERF2 nor MdERF3 Binds to the *MdACO1* Promoter.

Supplemental Figure 7. Yeast Two-Hybrid Assay Showing That MdMYC2 Does Not Interact with MdERF1 or MdERF3.

Supplemental Figure 8. The Interaction between MdMYC2 and MdERF2 Inhibits the Binding of MdMYC2 to the Promoters of *MdACS1* and *MdACO1*.

Supplemental Figure 9. Expression of *MdACSs* in MeJA-Treated Apple Fruit.

Supplemental Figure 10. ChIP-PCR Showing That MdERF3 Binds to the *MdMYC2* Promoter.

Supplemental Figure 11. MdERF2 and MdERF3 Compete with Each Other for Binding to the *MdACS1* Promoter.

Supplemental Data Set 1. List of Primers Used in This Study.

ACKNOWLEDGMENTS

This work was supported by the National Natural Science Foundation of China (31672121). We thank Zhi Liu (Institute of Pomology, Liaoning Academy of Agricultural Sciences, China) for providing apple fruits, Takaya Moriguchi (National Institute of Fruit Tree Science, Japan) for providing apple fruit callus, and Jianmin Zhou (Chinese Academy of Sciences) for providing the Luc vectors. We also thank PlantScribe (http://www.plantscribe.com/) for language editing.

AUTHOR CONTRIBUTIONS

A.W., T.L., and D.T. conceived and designed this research. T.L. performed most of the experiments. Y.X. and L.Z. generated the constructs for protein purification. Y.J. performed the qRT-PCR assay. H.Y. performed protein purification. T.L., D.T., and A.W. wrote the article. All authors analyzed the data and discussed the article.

Received May 3, 2017; revised May 16, 2017; accepted May 25, 2017; published May 26, 2017.

REFERENCES

Adams-Phillips, L., Barry, C., and Giovannoni, J. (2004). Signal transduction systems regulating fruit ripening. Trends Plant Sci. **9:** 331–338.

Barry, C.S., and Giovannoni, J.J. (2007). Ethylene and fruit ripening. J. Plant Growth Regul. **26:** 143–159.

Chen, H., Zou, Y., Shang, Y., Lin, H., Wang, Y., Cai, R., Tang, X., and Zhou, J.M. (2008). Firefly luciferase complementation imaging assay for protein-protein interactions in plants. Plant Physiol. **146:** 368–376.

Concha, C.M., Figueroa, N.E., Poblete, L.A., Oñate, F.A., Schwab, W., and Figueroa, C.R. (2013). Methyl jasmonate treatment induces changes in fruit ripening by modifying the expression of several ripening genes in *Fragaria chiloensis* fruit. Plant Physiol. Biochem. **70:** 433–444.

Dandekari, A.M., Teo, G., Defilippi, B.G., Uratsu, S.L., Passey, A.J., Kader, A.A., Stow, J.R., Colgan, R.J., and James, D.J. (2004). Effect of down-regulation of ethylene biosynthesis on fruit flavor complex in apple fruit. Transgenic Res. **13:** 373–384.

Fan, X., Mattheis, J.P., and Fellman, J.K. (1998). A role for jasmonates in climacteric fruit ripening. Planta **204:** 444–449.

Fan, X., Mattheis, J., Fellman, J., and Patterson, M. (1997). Effect of methyl jasmonate on ethylene and volatile production by summerred apples depends on fruit developmental stage. J. Agric. Food Chem. **45:** 208–211.

Fernández-Calvo, P., et al. (2011). The Arabidopsis bHLH transcription factors MYC3 and MYC4 are targets of JAZ repressors and act additively with MYC2 in the activation of jasmonate responses. Plant Cell **23:** 701–715.

Gapper, N.E., McQuinn, R.P., and Giovannoni, J.J. (2013). Molecular and genetic regulation of fruit ripening. Plant Mol. Biol. **82:** 575–591.

Giovannoni, J.J. (2004). Genetic regulation of fruit development and ripening. Plant Cell **16 (Suppl):** S170–S180.

Han, Y., Dang, R., Li, J., Jiang, J., Zhang, N., Jia, M., Wei, L., Li, Z., Li, B., and Jia, W. (2015). SUCROSE NONFERMENTING1-RELATED PROTEIN KINASE2.6, an ortholog of OPEN STOMATA1, is a negative regulator of strawberry fruit development and ripening. Plant Physiol. **167:** 915–930.

Han, Y.C., Kuang, J.F., Chen, J.Y., Liu, X.C., Xiao, Y.Y., Fu, C.C., Wang, J.N., Wu, K.Q., and Lu, W.J. (2016). Banana transcription factor MaERF11 recruits histone deacetylase MaHDA1 and represses the expression of MaACO1 and expansins during fruit ripening. Plant Physiol. **171:** 1070–1084.

Ireland, H.S., Yao, J.L., Tomes, S., Sutherland, P.W., Nieuwenhuizen, N., Gunaseelan, K., Winz, R.A., David, K.M., and Schaffer, R.J. (2013). Apple SEPALLATA1/2-like genes control fruit flesh development and ripening. Plant J. **73:** 1044–1056.

Ito, Y., Kitagawa, M., Ihashi, N., Yabe, K., Kimbara, J., Yasuda, J., Ito, H., Inakuma, T., Hiroi, S., and Kasumi, T. (2008). DNA-binding specificity, transcriptional activation potential, and the rin mutation effect for the tomato fruit-ripening regulator RIN. Plant J. **55:** 212–223.

Jia, H.F., Chai, Y.M., Li, C.L., Lu, D., Luo, J.J., Qin, L., and Shen, Y.Y. (2011). Abscisic acid plays an important role in the regulation of strawberry fruit ripening. Plant Physiol. **157:** 188–199.

Kazan, K., and Manners, J.M. (2013). MYC2: the master in action. Mol. Plant **6:** 686–703.

Kende, H. (1993). Ethylene biosynthesis. Annu. Rev. Plant Biol. **44:** 283–307.

Khan, A.S., and Singh, Z. (2015). Methyl jasmonate promotes fruit ripening and improves fruit quality in Japanese plum. J. Hortic. Sci. Biotechnol. **82:** 695–706.

Kim, W.T., Silverstone, A., Yip, W.K., Dong, J.G., and Yang, S.F. (1992). Induction of 1-aminocyclopropane-1-carboxylate synthase mRNA by auxin in mung bean hypocotyls and cultured apple shoots. Plant Physiol. **98:** 465–471.

Klee, H.J., and Giovannoni, J.J. (2011). Genetics and control of tomato fruit ripening and quality attributes. Annu. Rev. Genet. **45:** 41–59.

Kondo, S., Tomiyama, A., and Seto, H. (2000). Changes of endogenous jasmonic acid and methyl jasmonate in apples and sweet cherries during fruit development. J. Am. Soc. Hortic. Sci. **125:** 282–287.

Kondo, S., Meemak, S., Ban, Y., Moriguchi, T., and Harada, T. (2009). Effects of auxin and jasmonates on 1-aminocyclopropane-1-carboxylate (ACC) synthase and ACC oxidase gene expression during ripening of apple fruit. Postharvest Biol. Technol. **51:** 281–284.

Kotoda, N., Iwanami, H., Takahashi, S., and Abe, K. (2006). Antisense expression of MdTFL1, a TFL1-like gene, reduces the juvenile phase in apple. J. Am. Soc. Hortic. Sci. **131:** 74–81.

Lalel, H.J.D., Singh, Z., and Tan, S.C. (2015). The role of methyl jasmonate in mango ripening and biosynthesis of aroma volatile compounds. J. Hortic. Sci. Biotechnol. **78:** 470–484.

Li, T., Jiang, Z., Zhang, L., Tan, D., Wei, Y., Yuan, H., Li, T., and Wang, A. (2016). Apple (*Malus domestica*) MdERF2 negatively affects ethylene biosynthesis during fruit ripening by suppressing MdACS1 transcription. Plant J. **88:** 735–748.

Li, T., Li, X., Tan, D., Jiang, Z., Wei, Y., Li, J., Du, G., and Wang, A. (2014). Distinct expression profiles of ripening related genes in the 'Nanguo' pear (*Pyrus ussuriensis*) fruits. Sci. Hortic. (Amsterdam) **171:** 78–82.

Li, T., Tan, D., Liu, Z., Jiang, Z., Wei, Y., Zhang, L., Li, X., Yuan, H., and Wang, A. (2015). Apple MdACS6 regulates ethylene biosynthesis during fruit development involving ethylene-responsive factor. Plant Cell Physiol. **56:** 1909–1917.

Lin, Z., Zhong, S., and Grierson, D. (2009). Recent advances in ethylene research. J. Exp. Bot. **60:** 3311–3336.

Oraguzie, N.C., Iwanami, H., Soejima, J., Harada, T., and Hall, A. (2004). Inheritance of the Md-ACS1 gene and its relationship to fruit softening in apple (*Malus* x *domestica* Borkh.). Theor. Appl. Genet. **108:** 1526–1533.

Pauwels, L., et al. (2010). NINJA connects the co-repressor TOPLESS to jasmonate signalling. Nature **464:** 788–791.

Saniewski, M., and Czapski, J. (1985). Stimulatory effect of methyl jasmonate on the ethylene production in tomato fruits. Experientia **41:** 256–257.

Saniewski, M., Nowacki, J., and Czapski, J. (1987). The effect of methyl jasmonate on ethylene production and ethylene-forming enzyme activity in tomatoes. J. Plant Physiol. **129:** 175–180.

Schaffer, R.J., et al. (2007). A genomics approach reveals that aroma production in apple is controlled by ethylene predominantly at the final step in each biosynthetic pathway. Plant Physiol. **144:** 1899–1912.

Seymour, G.B., Østergaard, L., Chapman, N.H., Knapp, S., and Martin, C. (2013). Fruit development and ripening. Annu. Rev. Plant Biol. **64:** 219–241.

Sheard, L.B., et al. (2010). Jasmonate perception by inositol-phosphate-potentiated COI1-JAZ co-receptor. Nature **468:** 400–405.

Srivastava, A., and Handa, A.K. (2005). Hormonal regulation of tomato fruit development: a molecular perspective. J. Plant Growth Regul. **24:** 67–82.

Sunako, T., Ishikawa, R., Senda, M., Akada, S., Niizeki, M., and Harada, T. (2000). MdACS-5A (accession no. AB034992) and 5B (accession no. AB034993), two wound-responsive genes encoding 1-aminocyclopropane-1-carboxylate synthase in apple. Plant Physiol. **122:** 620.

Sunako, T., Sakuraba, W., Senda, M., Akada, S., Ishikawa, R., Niizeki, M., and Harada, T. (1999). An allele of the ripening-specific 1-aminocyclopropane-1-carboxylic acid synthase gene (ACS1) in apple fruit with a long storage life. Plant Physiol. **119:** 1297–1304.

Tan, D., Li, T., and Wang, A. (2013). Apple 1-aminocyclopropane-1-carboxylic acid synthase genes, MdACS1 and MdACS3a, are expressed in different systems of ethylene biosynthesis. Plant Mol. Biol. Report. **31:** 204–209.

Wakasa, Y., Kudo, H., Ishikawa, R., Akada, S., Senda, M., Niizeki, M., and Harada, T. (2006). Low expression of an endopolygalacturonase gene in apple fruit with long-term storage potential. Postharvest Biol. Technol. **39:** 193–198.

Wang, A., Tan, D., Takahashi, A., Li, T.Z., and Harada, T. (2007). MdERFs, two ethylene-response factors involved in apple fruit ripening. J. Exp. Bot. **58:** 3743–3748.

Wang, A., Yamakake, J., Kudo, H., Wakasa, Y., Hatsuyama, Y., Igarashi, M., Kasai, A., Li, T., and Harada, T. (2009). Null mutation of the MdACS3 gene, coding for a ripening-specific 1-aminocyclopropane-1-carboxylate synthase, leads to long shelf life in apple fruit. Plant Physiol. **151:** 391–399.

Wang, Z., Meng, D., Wang, A., Li, T., Jiang, S., Cong, P., and Li, T. (2013). The methylation of the PcMYB10 promoter is associated with green-skinned sport in Max Red Bartlett pear. Plant Physiol. **162:** 885–896.

Wiersma, P.A., Zhang, H., Lu, C., Quail, A., and Toivonen, P.M.A. (2007). Survey of the expression of genes for ethylene synthesis and perception during maturation and ripening of 'Sunrise' and 'Golden Delicious' apple fruit. Postharvest Biol. Technol. **44:** 204–211.

Xie, X.B., Li, S., Zhang, R.F., Zhao, J., Chen, Y.C., Zhao, Q., Yao, Y.X., You, C.X., Zhang, X.S., and Hao, Y.J. (2012). The bHLH transcription factor MdbHLH3 promotes anthocyanin accumulation and fruit colouration in response to low temperature in apples. Plant Cell Environ. **35:** 1884–1897.

Yang, S.F., and Hoffman, N.E. (1984). Ethylene biosynthesis and its regulation in higher plants. Annu. Rev. Plant Physiol. **35:** 155–189.

Yuan, H., Meng, D., Gu, Z., Li, W., Wang, A., Yang, Q., Zhu, Y., and Li, T. (2014). A novel gene, MdSSK1, as a component of the SCF complex rather than MdSBP1 can mediate the ubiquitination of S-RNase in apple. J. Exp. Bot. **65:** 3121–3131.

Zhang, X., Zhu, Z., An, F., Hao, D., Li, P., Song, J., Yi, C., and Guo, H. (2014). Jasmonate-activated MYC2 represses ETHYLENE INSENSITIVE3 activity to antagonize ethylene-promoted apical hook formation in Arabidopsis. Plant Cell **26:** 1105–1117.

Zhu, X., Chen, J., Xie, Z., Gao, J., Ren, G., Gao, S., Zhou, X., and Kuai, B. (2015). Jasmonic acid promotes degreening via MYC2/3/4- and ANAC019/055/072-mediated regulation of major chlorophyll catabolic genes. Plant J. **84:** 597–610.

Zhu, Z., et al. (2011). Derepression of ethylene-stabilized transcription factors (EIN3/EIL1) mediates jasmonate and ethylene signaling synergy in Arabidopsis. Proc. Natl. Acad. Sci. USA **108:** 12539–12544.